Electronic spectral function for a two-dimensional electron system in the fractional quantum Hall regime

Rudolf Haussmann*

Department of Physics, Indiana University, Swain Hall West 117, Bloomington, Indiana 47405

(Received 15 September 1995)

A two-dimensional system of interacting electrons is considered in a strong magnetic field in the fractional quantum Hall regime, where the motion of the electrons is restricted to the lowest Landau level in the lowest subband. Starting from a microscopic quantum-field theory we present a calculation of the electronic spectral function $A(\epsilon)$ for a single layer. From the original Coulomb interaction we separate an effective bosonic part, which is treated exactly by resummation of Feynman diagrams. For the electron Green's function $G(\tau - \tau')$, which is closely related to $A(\epsilon)$, we derive an approximate formula that goes beyond perturbation theory and is similar to the solution of an independent-boson model. The independent bosons are the collective excitations, mainly magnetorotons. Constructing a bosonic spectral function with the main features of the collective excitations by the single-mode approximation, we obtain a spectral function $A(\epsilon)$ with a double-peak structure and a pseudogap at $\epsilon \approx \mu$ for low temperatures. From this result we derive the current-voltage characteristic $I(V)$ for the tunneling of electrons between two layers, which shows a tunneling pseudogap for low temperatures and agrees with recent experiments.

I. INTRODUCTION

In recent experiments[1–3] concerning the tunneling between two layers of two-dimensional electron systems an unusual current-voltage characteristic $I(V)$ has been found at low temperatures $T \lesssim 1$ K if a strong perpendicular magnetic field is applied. It is possible to produce samples that are symmetric, so that both layers have nearly the same electron densities and properties. The magnetic field has been chosen to be so strong that the two electron layers are in the fractional quantum Hall regime, where only the lowest Landau level in the lowest subband is occupied with a fraction ν in the interval $0 < \nu < 1$ in each layer, respectively. The main observation is a tunneling pseudogap in the current-voltage characteristic $I(V)$ for low temperatures and high magnetic fields. The current I is strongly suppressed for small voltages V and nearly zero in the interval $0 \leq V \lesssim 2$ mV. For higher voltages $I(V)$ has a peak with a finite width, which is related to the tunneling between the lowest Landau levels of the lowest subbands. For much higher voltages there appear more peaks and structures in $I(V)$ which involve higher Landau levels and higher subbands in the tunneling process. However, we want to restrict our considerations to the tunneling between the lowest Landau levels of the lowest subbands and thus focus our attention on the first peak. A similar experiment,[4] which concerns the tunneling between a two-dimensional electron layer and a n^+ doped substrate, has also reported a strong suppression of the zero-voltage tunneling conductance for strong magnetic fields and low temperatures.

Thus, for low temperatures and high magnetic fields we have one peak in the current-voltage characteristic $I(V)$ occurring above an offset $V_0 \approx 2$ mV, below which the tunneling current is strongly suppressed (tunneling pseudogap). If we assume that the two layers are separated by a high and broad tunneling barrier so that the tunneling matrix element t is small and interactions between the layers can be neglected, then we can perform a linear-response calculation with respect to t and write the tunneling current from the left to the right layer as

$$I(V) = -e \frac{t^2 F}{\hbar \ell^2} \int d\epsilon [A_+^R(\epsilon - eV) A_-^L(\epsilon)$$
$$- A_+^L(\epsilon + eV) A_-^R(\epsilon)] \tag{1}$$

where F is the area of the tunneling contact and $\ell = (\hbar c / eB)^{1/2}$ is the magnetic length. Actually, the number of tunneling channels is $N_\Phi = F/2\pi\ell^2$. Here we have expressed the tunneling current in terms of the electronic spectral functions (Green's functions) $A_+(\epsilon)$ and $A_-(\epsilon)$ of electron and hole excitations, respectively. The upper index L or R means left or right layer and can be omitted because the two layers are made nearly equal.[1–3]

Since the samples are very pure and the mobilities are high, the effect is believed to arise from the strong correlations in the two-dimensional electron systems in the fractional quantum Hall regime while disorder plays a minor role. Eisenstein *et al.*[2] have shown that the interaction between the layers causes a small excitonic shift of the $I(V)$ peak to lower voltages and thus is also subsidiary. Thus, the main part of the effect should arise from the strong correlations in a single layer which is described by the density of states (the electronic spectral function) $A(\epsilon) = A_+(\epsilon) + A_-(\epsilon)$ of the lowest Landau level. Indeed the suppression of the current I for small voltages (the tunneling pseudogap) can be obtained from Eq. (1.1) if the electronic spectral function $A(\epsilon)$ is strongly suppressed in the close vicinity of the Fermi energy μ. This means that $A(\epsilon)$ should consist of two peaks [a hole peak $A_-(\epsilon)$ and an electron peak $A_+(\epsilon)$] separated by a pseudogap at $\epsilon = \mu$.

According to Eisenstein *et al.*[1] the double-peak structure of $A(\epsilon)$ can be explained easily on a qualitative level. Be-

cause of the strong correlations the two-dimensional electron liquids have a near ordering of the particles that is somewhat similar to a Wigner crystal. Thus, for the tunneling process one has to take out one electron from a "lattice place" of one layer and put it into an "interstitial place" of the other layer. This process costs a certain amount of energy, which produces an energy gap 2Δ in the density of states. Assuming a very short time for the tunneling process, the empty lattice place in the one layer will relax, and also the occupied interstitial place in the other layer will relax after a certain relaxation time by emitting collective modes like magnetophonons.

In order to bring these ideas to a quantitative level, Johansson and Kinaret[5] have developed a theory based on an independent-boson model.[6] They consider the tunneling process of a single electron from one layer into the other while the interaction with the other electrons is modeled by an interaction with collective excitations, the magnetophonons, which are treated as independent bosons. Using the spectrum of the magnetophonons in a Wigner crystal as an input, Johansson and Kinaret calculated the current-voltage characteristic $I(V)$ and obtained a quite good qualitative and quantitative agreement with the experiments. However, while the model of Johansson and Kinaret seems to be an easy explanation and yields good results, it appears to be somewhat artificially constructed and adjusted to the particular physical problem. Thus, it is necessary to find out why this model is good and to justify the model within the framework of a microscopic description.

Efros and Pikus[7] have applied a model of a classical electron liquid on a two-dimensional lattice to calculate the spectral function $A(\epsilon)$. They find the double-peak structure of $A(\epsilon)$ and the tunneling pseudogap of $I(V)$, and their results agree with the experiments. The spectral function $A(\epsilon)$ has also been calculated by numerical exact diagonalization of the Schrödinger equation for finite particle numbers $(N \leq 9)$.[8,9] However, recent more extensive calculations[9] have shown that the double-peak structure of $A(\epsilon)$ with the pseudogap at the Fermi energy μ is not found convincingly by this approach, probably because the particle number is too small. Aleiner, Baranger, and Glazman[10] have considered the spectral function $A(\epsilon)$ of a two-dimensional electron liquid in a weak magnetic field. Approximating the collective excitations by a hydrodynamic model, they find a pseudogap of $A(\epsilon)$ even for $\nu \gg 1$.

In this paper we consider the two-dimensional layer of interacting electrons in a strong perpendicular magnetic field on a microscopic level using the many-particle quantum-field theory.[11,12] The magnetic field should be so strong that the system is in the fractional quantum Hall regime with an occupation fraction ν in the interval $0 < \nu < 1$. We restrict the motion of the electrons to the lowest Landau level and assume spin polarization. Furthermore, we assume a high and broad tunneling barrier so that the interaction between the layers can be neglected and the tunneling current $I(V)$ is given by Eq. (1.1) in terms of single-layer electronic spectral functions. In Sec. II we describe the microscopic system and derive the Feynman rules. In Sec. III we consider the perturbation theory for the electron Green's function G and show that it fails even in the self-consistent version. The problem arises from the Dyson equation, which requires a *diverging*

spectrum for the self-energy Σ to obtain a spectral function $A(\epsilon)$ with double-peak structure and a pseudogap at $\epsilon \approx \mu$. Thus we must go beyond perturbation theory. In Sec. IV we present a method for a resummation of the Feynman diagrams that is closely related to the way to solve the independent-boson model[6] by field-theoretic means. We split the interaction between the electrons into a bosonic part with zero wave vector and a remaining part. While the original Coulomb interaction is instantaneous, the separated bosonic part is time dependent and contains retardation effects. We prove some exact theorems mainly based on local gauge invariance and particle conservation of the original interaction, which allow us to separate the bosonic part of the interaction as an exponential factor. Thus we can express the electron Green's function G in terms of the bosonic exponential factor, which can be calculated exactly, and a Green's function $\tilde{G}$, which depends only on the remaining part of the interaction.

The bosonic interaction part is arbitrary at first and should be chosen and adjusted in such a way that the remaining Green's function $\tilde{G}$ can be calculated perturbatively. This is done in Sec. V. In a first-order self-consistent approximation we obtain a free Green's function for $\tilde{G}$ with shifted energy, while the bosonic part of the interaction is mainly an integral of the density-density correlation function over the wave vector. In this way we obtain an electron Green's function G that has exactly the form of the solution of the independent-boson model. Here the independent bosons are the collective excitations described by the density-density correlation function. It turns out that the double-peak structure of the spectral function $A(\epsilon)$ is produced by the bosonic exponential factor of G if the collective excitations have their main spectral weight at low energies below $0.15 e^2/\ell$. In Sec. VI we use the single-mode approximation[13] to determine the spectrum of the collective excitations. It turns out that the main spectral weight arises from the magnetorotons. We then take this bosonic spectrum as an input and calculate the electronic spectral function $A(\epsilon)$ and the current-voltage characteristic $I(V)$. We find agreement with the experiments.[1–3] While our theory and result are somewhat different, we mainly confirm the approach of Johansson and Kinaret[5] by a systematic approximation starting from a microscopic quantum-field theory.

II. MICROSCOPIC THEORY AND THE RELATED FEYNMAN RULES

We consider a two-dimensional system of interacting electrons moving in the xy plane, where a perpendicular magnetic field B in z direction is applied. The system is described by the Hamiltonian

$$\hat{H} = \int d^2r \frac{1}{2m} \left\{ \left| \left(p_x + \frac{e}{c} A_x \right) \hat{\psi}(\mathbf{r}) \right|^2 + \left| \left(p_y + \frac{e}{c} A_y \right) \hat{\psi}(\mathbf{r}) \right|^2 \right\}$$
$$+ \frac{1}{2} \int d^2r \int d^2r' : [\hat{\rho}(\mathbf{r}) - \rho_b] V(\mathbf{r} - \mathbf{r}') [\hat{\rho}(\mathbf{r}') - \rho_b]:$$

$$(2.1)$$

where $\hat{\psi}(\mathbf{r})$ and $\hat{\psi}^+(\mathbf{r})$ are the fermion field operators and $\hat{\rho}(\mathbf{r}) = \hat{\psi}^+(\mathbf{r}) \hat{\psi}(\mathbf{r})$ is the operator of the electron density. The

two colons :: mean that the product in between has to be normal ordered with respect to the fermion operators. In circular gauge the vector potential is given by $A_x = -\frac{1}{2}By$ and $A_y = \frac{1}{2}Bx$. The electrons interact via the Coulomb potential $V(\mathbf{r}) = e^2/|\mathbf{r}|$. The subtraction of the homogeneous density $\rho_b = \nu/2\pi\ell^2$ in the interaction term means that we assume a neutralizing positively charged background. We assume that the electrons are spin polarized and that their motion is restricted to the lowest Landau level. Thus, we can expand the fermion field operators in the form

$$\hat{\psi}(\mathbf{r}) = \sum_m \varphi_m(\mathbf{r})\hat{c}_m, \quad \hat{\psi}^+(\mathbf{r}) = \sum_m \varphi_m^*(\mathbf{r})\hat{c}_m^+, \quad (2.2)$$

where $\hat{c}_m$ and $\hat{c}_m^+$ are operators satisfying fermion commutation relations and $\varphi_m(\mathbf{r})$ are the orthonormalized single-particle basis functions of the lowest Landau level. The index m counts the degrees of freedom of the degeneracy of the lowest Landau level. In our considerations we need not specify a particular choice of the degenerate single-particle functions $\varphi_m(\mathbf{r})$.

The perturbation series expansion of the interacting electron system in a strong magnetic field in terms of Feynman diagrams has been considered previously by Zheng and MacDonald.[14] We use the formalism of many-particle quantum-field theory with temperature-dependent Green's functions.[11,12,15] The object of basic interest is the fermion Green's function

$$G_{mm'}(\tau - \tau') = \langle T[\hat{c}_m(\tau)\hat{c}_{m'}^+(\tau')]\rangle, \quad (2.3)$$

where τ is the temperature parameter that corresponds to an imaginary time and varies in the interval $0 \leq \tau \leq \hbar\beta = \hbar/k_B T$. By $T[\cdots]$ we understand the usual time-ordered product with respect to τ. Since the magnetic field is homogeneous, the system is translationally invariant in the xy plane up to a phase factor in the wave function. This implies that the fermion Green's function (2.3) is proportional to a unit matrix with respect to the degenerate degrees of freedom,

$$G_{mm'}(\tau - \tau') = \delta_{mm'}G(\tau - \tau'). \quad (2.4)$$

We define the Fourier-transformed Green's function $G(\omega_n)$ by

$$G(\tau) = \frac{1}{\beta}\sum_{\omega_n} e^{-i\omega_n\tau}G(\omega_n) \quad (2.5)$$

where $\omega_n = \pi(2n+1)/\hbar\beta$ are the fermionic Matsubara frequencies. $G(\omega_n)$ can be expressed in terms of $A(\epsilon)$ by the spectral representation

$$G(\omega_n) = \int d\epsilon \frac{A(\epsilon)}{-i\hbar\omega_n + \epsilon - \mu}. \quad (2.6)$$

where μ is the chemical potential. Thus, we can obtain the spectral function $A(\epsilon)$ from the electron Green's function by an analytic continuation of $G(\omega_n)$ to continuous complex frequencies. Finally, the current-voltage characteristic $I(V)$ is obtained from (1.1).
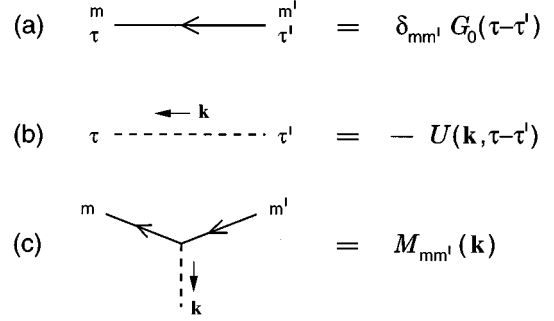

FIG. 1. Basic elements of the Feynman diagrams: (a) free fermion Green's function, (b) interaction line, and (c) 3 vertex connecting fermion and interaction lines.

The collective excitations are represented by the connected density-density correlation function

$$\chi_{\rho\rho}(\mathbf{r} - \mathbf{r}', \tau - \tau') = \langle T[\hat{\rho}(\mathbf{r}, \tau)\hat{\rho}(\mathbf{r}', \tau')]\rangle_c, \quad (2.7)$$

where $\hat{\rho}(\mathbf{r}, \tau) = \hat{\psi}^+(\mathbf{r}, \tau)\hat{\psi}(\mathbf{r}, \tau)$. The Fourier-transformed function $\chi_{\rho\rho}(\mathbf{k}, \Omega_n)$ is defined by

$$\chi_{\rho\rho}(\mathbf{r}, \tau) = \int \frac{d^2k}{(2\pi)^2} \frac{1}{\beta}\sum_{\Omega_n} e^{i(\mathbf{kr} - \Omega_n\tau)}\chi_{\rho\rho}(\mathbf{k}, \Omega_n), \quad (2.8)$$

where $\mathbf{k}$ is the wave vector of the collective excitations and $\Omega_n = 2\pi n/\hbar\beta$ are the bosonic Matsubara frequencies. In analogy to (2.6) the spectral function $\chi_{\rho\rho}''(\mathbf{k}, \epsilon)$ of the collective excitations is defined by

$$\chi_{\rho\rho}(\mathbf{k}, \Omega_n) = \int d\epsilon \frac{\chi_{\rho\rho}''(\mathbf{k}, \epsilon)}{-i\hbar\Omega_n + \epsilon}. \quad (2.9)$$

The functions $G(\tau - \tau')$ and $\chi_{\rho\rho}(\mathbf{k}, \tau - \tau')$ can be calculated by a perturbation series expansion in terms of Feynman diagrams. We now describe the rules and the basic elements by which the diagrams can be constructed. In Fig. 1(a) we associate the free Green's function

$$G_{0,mm'}(\tau - \tau') = \delta_{mm'}[\theta(\tau - \tau') - n(\epsilon_0)]$$
$$\times \exp\{-\hbar^{-1}(\epsilon_0 - \mu)(\tau - \tau')\}$$
$$(2.10)$$

with a directed full line where ϵ_0 is the single-particle energy of the lowest Landau level and $n(\epsilon) = 1/[e^{\beta(\epsilon - \mu)} + 1]$ is the Fermi distribution function. It is convenient to introduce the imaginary time-dependent interaction

$$U(\mathbf{k}, \tau - \tau') = V(\mathbf{k})\hbar\sum_n \delta(\tau - \tau' + n\hbar\beta), \quad (2.11)$$

which we identify in Fig. 1(b) with a dashed line. Here $V(\mathbf{k}) = e^2 2\pi/|\mathbf{k}|$ is the two-dimensional Fourier transform of the Coulomb potential. The delta function in (2.11) represents the fact that the Coulomb interaction is instantaneous. However, our following considerations are not restricted to an instantaneous interaction. They remain valid also for a nontrivial time-dependent interaction $U(\mathbf{k}, \tau - \tau')$ including retardation effects as, e.g., the electron-phonon interaction.
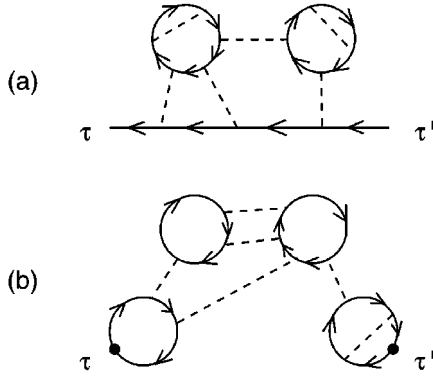
FIG. 2. Typical Feynman diagrams of (a) the fermion Green's function $G(\tau - \tau')$ and (b) the connected density-density correlation function $\chi_{\rho\rho}(\mathbf{k}, \tau - \tau')$.

The full fermion lines and the dashed interaction lines are connected by a 3 vertex which is shown in Fig. 1(c). While in real space the 3 vertex is local, in our representation it is associated with the matrix element

$$M_{mm'}(\mathbf{k}) = \int d^2 r\, \varphi_m^*(\mathbf{r})\, e^{i\mathbf{k}\mathbf{r}}\, \varphi_{m'}(\mathbf{r}). \qquad (2.12)$$

Since the particular representation of the degenerate degrees of freedom m is irrelevant, we do not need the explicit form of $M_{mm'}(\mathbf{k})$. Thus, we can omit the indices m, m' and consider $M(\mathbf{k})$ as a matrix. All we need are some formulas that define the algebra of these matrices. From any particular representation we derive

$$M(\mathbf{k}_1) \cdot M(\mathbf{k}_2) = \exp[\tfrac{1}{2}\kappa_1^* \kappa_2 \ell^2] M(\mathbf{k}_1 + \mathbf{k}_2), \qquad (2.13a)$$

$$M(\mathbf{0}) = 1, \qquad (2.13b)$$

$$\mathrm{Tr}[M(\mathbf{k})] = [2\pi\ell^2]^{-1}(2\pi)^2 \delta(\mathbf{k}), \qquad (2.13c)$$

where $\kappa = k_x + i k_y$ is the complex representation of the wave vector $\mathbf{k}$ and $\ell = (\hbar c/eB)^{1/2}$ is the magnetic length. The Feynman diagrams of the perturbation series are constructed in all possible ways from the basic elements of Fig. 1. The sums over the indices m of the degenerate degrees of freedom can be evaluated with the three formulas of (2.13). For each 3 vertex we must perform an imaginary-time integral $\int_0^{\hbar\beta} d\tau/\hbar$, and for each dashed interaction line we must perform a wave-vector integral $\int d^2 k/(2\pi)^2$. Finally, it turns out that all Hartree-type subdiagrams are canceled by the positively charged neutralizing background, if we choose $\rho_b = \nu/2\pi\ell^2$ where $\nu = -G(\tau = -0)$ is the occupation fraction of the lowest Landau level.

In Fig. 2(a) we show a typical diagram of the fermion Green's function $G(\tau - \tau')$. It consists of one open fermion line from τ' to τ and a certain number of closed fermion loops that are connected in any possible way by dashed interaction lines. In Fig. 2(b) we show a typical diagram of the connected density-density correlation function $\chi_{\rho\rho}(\mathbf{k}, \tau - \tau')$, which consists of a certain number of closed fermion loops connected in any possible way by dashed interaction lines. Thus, the functions $G(\tau - \tau')$ and

$\chi_{\rho\rho}(\mathbf{k}, \tau - \tau')$ are given by the sums of all possible diagrams with structures shown in Figs. 2(a) and 2(b), respectively.

III. FAILURE OF PERTURBATION THEORY

For an interacting two-dimensional electron system in a strong magnetic field B perturbation theory is problematic because of the degeneracy of the Landau levels. If the lowest Landau level is only partially filled with an occupation fraction ν in the interval $0 < \nu < 1$, the noninteracting ground state is degenerate and standard perturbation theory does not work for small temperatures. Let us assume that ν is not too close to 0 or 1. Then the average distance between the electrons is of order of the magnetic length $\ell = (\hbar c/eB)^{1/2}$. Hence the interaction energy per electron is of order e^2/ℓ. The quantum-field theory with temperature-dependent Green's functions that we have described in Sec. II is an expansion with respect to powers of the dimensionless parameter $\alpha = \beta e^2/\ell$. (The factor $\beta = 1/k_B T$ arises from the integral over τ for each vertex.) Since α must be small, this perturbation theory is a high-temperature expansion that is good for $T \gg k_B^{-1} e^2/\ell$. However, the experiments[1–3] that measure the tunnel current $I(V)$ are performed at low temperatures. It turns out that for these experiments the expansion parameter is of order $\alpha \sim 100$ (where we take a dielectric constant $\epsilon \approx 13$ into account) so that standard perturbation theory truncated at finite order is not applicable.

Thus, in order to explain the experiments we must go beyond perturbation theory. This means we must resum at least a certain class of diagrams (or, if we are unlucky, even all diagrams). One possibility is to express the electron Green's function $G(\omega_n)$ via the Dyson equation,

$$G(\omega_n) = 1/[-i\hbar\omega_n + \epsilon_0 - \mu - \Sigma(\omega_n)], \qquad (3.1)$$

in terms of the self-energy $\Sigma(\omega_n)$. Summing over all self-energy subdiagrams in the diagrams of $\Sigma(\omega_n)$, the self-energy $\Sigma(\omega_n)$ becomes a functional of the exact electron Green's function. Actually, the self-energy can be expressed in terms of the functional derivative,[11,16]

$$\Sigma(\omega_n) = -\delta\Phi[G]/\delta G(\omega_n), \qquad (3.2)$$

where $\Phi[G]$ is a functional of $G(\omega_n)$ given by the series of all connected vacuum diagrams without self-energy subdiagrams, where the propagator lines are identified with the exact $G(\omega_n)$. In this way the quantum-field theory becomes self consistent. The electron Green's function $G(\omega_n)$ can be determined by solving Eqs. (3.1) and (3.2) iteratively. Approximations are made in the functional $\Phi[G]$ by taking into account only certain classes of diagrams. Thus the ladder approximation and the random-phase approximation (RPA) are found by considering only ring diagrams with ladders or with bubble chains, respectively.

The self-consistent quantum-field theory has been successfully applied to Fermi liquids and superconductivity. Recently, this theory has been found to be the appropriate approach to describe the crossover from BCS superconductivity to Bose-Einstein condensation in a strongly interacting electron liquid.[17] Thus, it is very challenging to apply this approach also to the present problem of the two-dimensional electron system in the fractional quan-

tum Hall regime. Unfortunately, it turns out that this approach fails too. We want to describe why and in which way it fails. The identification of the propagator lines with the exact Green's function $G(\omega_n)$ implies that the self-consistent perturbation series is no more a power series in α so that the diagrams remain finite in the limit $T \to 0$, $\alpha \to \infty$. This is already progress. However, it turns out that the diagrams are all of the same order so that we cannot make an approximation for $\Phi[G]$ but must sum *all* diagrams, which is an impossible task.

We have solved the self-consistent equations (3.1) and (3.2) numerically with functionals $\Phi[G]$ in ladder approximation, in RPA, and in a combination of RPA with the particle-hole ladder. In all three cases we obtain qualitatively similar results, so that we report here only about the RPA (because the RPA takes the screening of the Coulomb potential into account). The explicit form of the self-consistent equations can be derived in a way similar to that of as it has been done in Ref. 17 for superconductivity. The main change is that here we must use the Feynman rules of Sec. II and that in this case no space variable occurs because the motion of the electrons is restricted to the lowest Landau level. (In a homogeneous system the space dependence factorizes and can be separated.) Thus, in RPA the self-energy can be written as

$$\Sigma(\tau) = G(\tau)\Gamma(\tau), \qquad (3.3)$$

where $\Gamma(\tau)$ is the RPA vertex function given by

$$\Gamma(\Omega_n) = 2\pi\ell^2 \int \frac{d^2k}{(2\pi)^2} \frac{\lambda(\mathbf{k})}{1 + \lambda(\mathbf{k})\chi(\Omega_n)}. \qquad (3.4)$$

Here, $\lambda(\mathbf{k}) = (2\pi\ell^2)^{-1}\exp\{-(1/2)\mathbf{k}^2\ell^2\}V(\mathbf{k})$ is the effective interaction in Fourier representation and

$$\chi(\tau) = -G(-\tau)G(\tau) \qquad (3.5)$$

is the particle-hole pair propagator. [We note that the pair propagator $\chi(\tau)$ and the connected density-density correlation function $\chi_{\rho\rho}(\mathbf{r},\tau)$ (2.7), are two different quantities that should not be confused.] We have solved the self-consistent equations (3.1) and (3.3)–(3.5) numerically by iteration. To do this we need an efficient numerical Fourier transformation to transform the functions from the imaginary-time representation to the Matsubara-frequency representation. We have described such a numerical procedure in the Appendix of the second paper of Ref. 17. Then, to obtain the spectral functions $A(\epsilon)$ and $\chi''(\epsilon)$ related to $G(\omega_n)$ and $\chi(\Omega_n)$ we perform a numerical analytic continuation using Padé approximation. [$\chi''(\epsilon)$ is defined by an equation analogous to (2.9).] It turns out that for two identical layers the current-voltage characteristic (1.1) can be written exactly in terms of the spectral function $\chi''(\epsilon)$ of the pair propagator as

$$I(V) = e\frac{t^2 F}{\hbar\ell^2}\chi''(eV). \qquad (3.6)$$

One should note that $\chi''(\epsilon) = -\chi''(-\epsilon)$ is always antisymmetric so that $I(-V) = -I(V)$, as it should be.

Since the numerical analytical continuation fails sometimes and can give inaccurate results (especially for higher temperatures), it is useful to transform the self-consistent
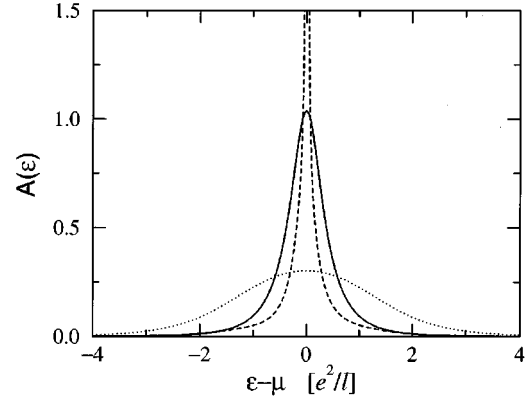

FIG. 3. The electronic spectral function $A(\epsilon)$ in self-consistent RPA for $T = \infty$ ($\alpha = 0$, dotted line), $T = k_B^{-1}e^2/\ell$ ($\alpha = 1$, full line), and $T = 0.01 k_B^{-1}e^2/\ell$ ($\alpha = 100$, dashed line).

equations (3.1)–(3.5) into a real-time and real-frequency representation that deals directly with the spectral functions. This can be done by using the Keldysh formalism[18,19] in thermal equilibrium. The resulting self-consistent equations look formally similar to (3.1)–(3.5) and are not more complicated. We have solved these latter equations also numerically by iteration and Fourier transformation. It turns out that for low temperatures $T \lesssim k_B^{-1}e^2/\ell$ and $\alpha \gtrsim 1$ the Matsubara formalism combined with the analytic continuation works better and is accurate while for high temperatures $T \gtrsim k_B^{-1}e^2/\ell$ and $\alpha \lesssim 1$ the Keldysh formalism must be used. In the overlap region where $\alpha \sim 1$ both methods yield nearly the same results for the spectral functions with an accuracy of 10^{-3}. Thus, we are able to solve the self-consistent equations with a very high numerical accuracy for $A(\epsilon)$ and $\chi''(\epsilon)$ in the parameter range $0 \leq \alpha \leq 1000$.

In Fig. 3 we show our results for the electronic spectral function $A(\epsilon)$. We choose for convenience always $\nu = 1/2$. The results remain qualitatively the same also for other occupation fractions ν not too close to 0 or 1 except that $A(\epsilon)$ is no more symmetric. Peculiarities at certain rational fractions $\nu = p/q$ are not seen. Thus, for the intermediate temperature $T = k_B^{-1}e^2/\ell$, which corresponds to $\alpha = 1$, we obtain one broad peak (full line). If we increase the temperature (decrease α) the peak becomes broader and lower. For $T \gtrsim 3k_B^{-1}e^2/\ell$ (or $\alpha \lesssim 1/3$) the curve nearly does not change any more until $T = \infty$ (or $\alpha = 0$) is reached (see dotted line). Since the peak (dotted line) has a finite width, the self-consistent quantum-field theory turns out to be nontrivial even for infinite temperatures where $\alpha = 0$. On the other hand, if we lower the temperature T below $k_B^{-1}e^2/\ell$ where we come into the region $\alpha > 1$, the peak becomes narrower and higher, until it diverges at the Fermi energy $\epsilon = \mu$ for $T \to 0$. This behavior is clearly shown in Fig. 3 by the dashed line, which we calculated for $T = 0.01 k_B^{-1}e^2/\ell$ and $\alpha = 100$. The numerical result indicates a divergence $A(\epsilon) \sim |\epsilon - \mu|^{-1/2}$ for ϵ close to μ and for $T = 0$, which can be derived also analytically from the self-consistent equations (3.1) and (3.3)–(3.5) by considering the asymptotic behavior of the functions. This divergence contradicts the experimental results[1–3] from which one expects the *opposite*
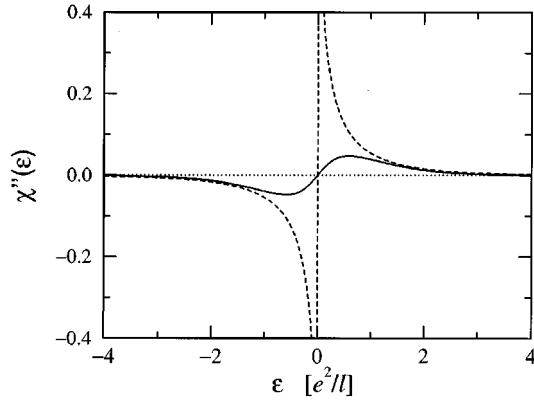
FIG. 4. The spectral function of the particle-hole pair propagator $\chi''(\epsilon)$ [directly related to the current voltage characteristic $I(V)$ by (3.6)] in self-consistent RPA for $T = \infty$ ($\alpha = 0$, dotted line), $T = k_B^{-1} e^2 / \ell$ ($\alpha = 1$, full line), and $T = 0.01 k_B^{-1} e^2 / \ell$ ($\alpha = 100$, dashed line).

for $A(\epsilon)$: for low temperatures the electronic spectral function $A(\epsilon)$ should be *suppressed* close to $\epsilon = \mu$ and form a pseudogap.

Thus, the self-consistent quantum-field theory fails for low temperatures. It turns out that if we lower the temperature more and more (where $\alpha > 1$ is increased) the numerical iteration procedure becomes unstable. This fact might be viewed as an indication of the failure of the theory for low temperatures. To make the iteration convergent we must slow it down, and thus we can solve the equations also for very low temperatures up to $\alpha \sim 1000$. In Fig. 4 we show the spectral function of the pair propagator $\chi''(\epsilon)$, which is directly related to the current-voltage characteristic $I(V)$ by (3.6). The results for intermediate and high temperatures (full and dotted line) seem to be reasonable. However, the result for low temperatures (dashed line, with $\alpha = 100$ of the same order as in the experiments) clearly contradicts the experiments.[1–4] We predict that for low temperatures $I(V)$ diverges for small voltages V, while the experiments have measured a pseudogap with a strong suppression of $I(V)$ for small V. Thus we come to the conclusion that the self-consistent quantum-field theory cannot explain the tunneling experiments.

If the exact electron Green's function $G(\omega_n)$ is known, one has two possibilities to calculate the related self-energy $\Sigma(\omega_n)$: first, the Dyson equation (3.1) used in backward direction and second, the self-consistent perturbation series (3.2). In an exact theory both equations must yield the same result. By an analytical continuation we can state similar equations for the electronic spectral function $A(\epsilon)$ and the spectral function of the self-energy $\Sigma''(\epsilon)$. [Here $\Sigma''(\epsilon)$ is defined similarly to $A(\epsilon)$ by an equation analogous to (2.6) for the self-energy. It turns out that the relation between $A(\epsilon)$ and $\Sigma''(\epsilon)$ arising from the Dyson equation does not depend on the temperature.] From the experimental findings it is believed that at low temperatures the exact electronic spectral function $A(\epsilon)$ has two broad peaks separated by a pseudogap at $\epsilon \approx \mu$. In Fig. 5(a) a typical spectral function $A(\epsilon)$ of this kind is shown. For simplicity we model $A(\epsilon)$ by two Gaussian peaks and assume the occupation fraction $\nu = 1/2$ so that $A(\epsilon)$ is symmetric around $\epsilon = \mu$. The Dyson
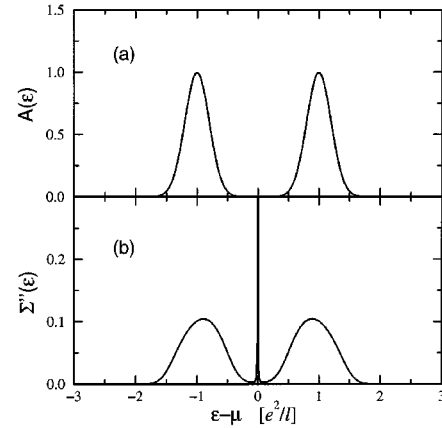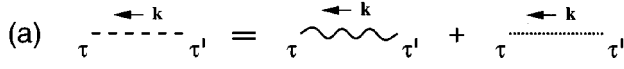

FIG. 5. (a) Electronic spectral function $A(\epsilon)$ as expected from the experiments. For simplicity we have assumed $\nu = 1/2$ and modeled $A(\epsilon)$ by two Gaussian peaks. (b) Spectral function of the self energy $\Sigma''(\epsilon)$ obtained via the Dyson equation (3.1) together with (2.6) from $A(\epsilon)$. The main feature is the very narrow peak at $\epsilon \approx \mu$, which is related to the pseudogap of $A(\epsilon)$ at $\epsilon \approx \mu$.

equation (3.1) can be handled easily and yields the exact self-energy if the exact Green's function is known. In this way the spectral function of the self-energy $\Sigma''(\epsilon)$ shown in Fig. 5(b) is obtained. The curve in Fig. 5(b) can be viewed as the exact spectral function $\Sigma''(\epsilon)$ if Fig. 5(a) is exact. Clearly, this curve shows the main feature of $\Sigma''(\epsilon)$ related to the pseudogap of $A(\epsilon)$ at $\epsilon \approx \mu$: $\Sigma''(\epsilon)$ has a very narrow peak at $\epsilon \approx \mu$ that is nearly a delta function. Alternatively, $\Sigma''(\epsilon)$ can be determined from $A(\epsilon)$ by the self-consistent perturbation series (3.2), which can be treated only approximately. To construct a successful self-consistent quantum-field theory one must find for $\Phi[G]$ such an approximation that the resulting spectral function $\Sigma''(\epsilon)$ looks at least qualitatively similar to that in Fig. 5(b) with the essential features. However, any approximation we have tried (RPA and ladder approximation) was not successful. While we find the two broad peaks, from (3.2) we never obtain the very narrow peak of $\Sigma''(\epsilon)$ at $\epsilon \approx \mu$ that is essential for the occurrence of the pseudogap in $A(\epsilon)$.

IV. BEYOND PERTURBATION THEORY: SEPARATION OF A BOSONIC FACTOR FROM THE ELECTRON GREEN'S FUNCTION

Now, we want to present an approach that goes beyond perturbation theory and covers the essential physics of the effect. From the qualitative discussion of Eisenstein *et al.* [1] and the theory of Johansson and Kinaret[5] it has become clear that the independent-boson model[6] of one electron in the two-dimensional layer coupled to the collective excitations seems to be the correct picture, in a very rough form, about what is going on in the tunneling experiment. In this section we present a special procedure of reordering the Feynman diagrams of the perturbation series that can be viewed as the field-theoretic method of how to derive the exact solution of the independent-boson model. We develop this method for the two-dimensional interacting electron system in the fractional quantum Hall regime, which we have described in Sec. II. In the next section we derive an approximate formula for the electron Green's function that looks similar to the solu-

(b) $- U(\mathbf{k}, \tau - \tau') = (2\pi)^2 \delta(\mathbf{k}) \Delta B(\tau - \tau') - \tilde{U}(\mathbf{k}, \tau - \tau')$

FIG. 6. Separation of the interaction (dashed line) into a bosonic part (wavy line) and a remaining part (dotted line), shown (a) diagrammatically and (b) in terms of formulas.

tion of the independent-boson model.

The basic idea is to split the interaction $U(\mathbf{k}, \tau - \tau')$ into two contributions, a bosonic part

$$- (2\pi)^2 \delta(\mathbf{k}) \Delta B(\tau - \tau'), \qquad (4.1)$$

which carries no momentum but is time dependent and may contain retardation effects, and a remaining part $\tilde{U}(\mathbf{k}, \tau - \tau')$. Diagrammatically and in terms of the related formulas this is shown in Fig. 6. [We assume that 3 vertices are constructed with wavy lines and dotted lines as done with the dashed line in Fig. 1(c).] The nontrivial part of the interaction is the bosonic part (wavy line), which we want to separate from the perturbation series and treat exactly. For the proofs of the theorems in this section we need the following two assumptions. First, in real space the boson Green's function $\Delta B(\tau - \tau')$ (wavy line) should not depend on the space coordinate. In Fourier space this assumption implies the factor $(2\pi)^2 \delta(\mathbf{k})$ in (4.1), which means that the bosons carry no momentum. Secondly, we assume

$$\Delta B(\Omega_n = 0) = \hbar^{-1} \int_0^{\hbar \beta} d\tau' \Delta B(\tau - \tau') = 0. \qquad (4.2)$$

While the original interaction (dashed line) is instantaneous, the bosonic part (wavy line) is nonlocal in time and contains retardation effects. However, $\Delta B(\tau - \tau')$ may contain also instantaneous contributions that are delta functions in time. Thus, it is convenient to introduce the *continuous* contribution $B(\tau - \tau')$ from which all delta functions are separated, defined by

$$\Delta B(\tau - \tau') = B(\tau - \tau') - 2\Delta \sum_{n=-\infty}^{+\infty} \hbar \delta(\tau - \tau' + n\hbar\beta). \qquad (4.3)$$
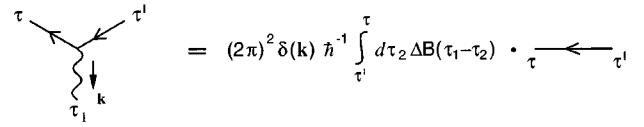
Here 2Δ is a constant which will later be identified as an energy gap. While at the moment the continuous bosonic function $B(\tau - \tau')$ is arbitrary and may be anything, the constant 2Δ is fixed by our second assumption (4.2) and must be chosen as

$$2\Delta = \hbar^{-1} \int_0^{\hbar \beta} d\tau B(\tau) = B(\Omega_n = 0). \qquad (4.4)$$

In this way we can be sure that (4.2) is always satisfied. Since the interaction lines are not directed, we can assume that the bosonic function is symmetric,

$$B(\tau - \tau') = B(\tau' - \tau) \qquad (4.5)$$

(otherwise it could be symmetrized). Furthermore, any bosonic Green's function is periodic in the imaginary time,

FIG. 7. Theorem 1: factorization of the 3 vertex with a wavy line. This equation is valid under the two assumptions that the wavy line carries only zero momentum [i.e., it is proportional to $(2\pi)^2 \delta(\mathbf{k})$] and that $\Delta B(\Omega_n = 0) = 0$ [Eq. (4.2)].

$$B(\tau - \tau' + n\hbar\beta) = B(\tau - \tau') \text{ for } n \in \mathbb{Z}. \qquad (4.6)$$

An important function, which appears in our theorems, is defined by the integral

$$\Delta \Phi(\tau - \tau') = \frac{1}{2} \hbar^{-2} \int_{\tau'}^{\tau} d\tau_1 \int_{\tau'}^{\tau} d\tau_2 \Delta B(\tau_1 - \tau_2)$$

$$= \hbar^{-2} \int_0^{\tau - \tau'} d\tau_1 \int_0^{\tau_1} d\tau_2 \Delta B(\tau_2). \qquad (4.7)$$

This function is also symmetric and because of (4.2) also periodic. Hence $\Delta \Phi(\tau - \tau')$ is also a bosonic function with the properties (4.5) and (4.6). Evaluating the integral over the delta functions explicitly, we obtain

$$\Delta \Phi(\tau - \tau') = -\hbar^{-1} \Delta |\tau - \tau'| + \hbar^{-2} \int_0^{\tau - \tau'} d\tau_1 \int_0^{\tau_1} d\tau_2 B(\tau_2) \qquad (4.8)$$

for $0 \leq \tau, \tau' \leq \hbar\beta$.

Now, let us turn back to the Feynman diagrams of the electron Green's function $G(\omega_n)$ and of the connected density-density correlation function $\chi_{\rho\rho}(\mathbf{k}, \Omega_n)$. We split the interaction (dashed line) as described above into a boson mediated part (wavy line) and a remaining part (dotted line). Then we obtain Feynman diagrams consisting of fermion lines which are connected by wavy lines and by dotted lines in any possible way. What changes in the diagrams of Fig. 2 is that now two types of interaction lines occur, wavy and dotted lines instead of the original dashed lines.

Let us now consider a 3 vertex with two free electron Green's functions and a wavy line. The two assumptions that we have made above allow us to prove Theorem 1, which states that the 3 vertex decomposes into a product of an integral of the bosonic function $\Delta B(\tau - \tau')$ and a single electron Green's function. In Fig. 7 the theorem is formulated in terms of Feynman diagrams. For the 3 vertex on the left-hand side we write down the expression

$$\hbar^{-1} \int_0^{\hbar \beta} d\tau_2 (2\pi)^2 \delta(\mathbf{k}) \Delta B(\tau_1 - \tau_2)$$

$$\times G_0(\tau - \tau_2) M(-\mathbf{k}) G_0(\tau_2 - \tau'). \qquad (4.9)$$

Because of the factor $(2\pi)^2 \delta(\mathbf{k})$ and the formula (2.13b) we can substitute $M(-\mathbf{k}) \to M(\mathbf{0}) = 1$, which can be absorbed in one of the free Green's functions. Then, inserting (2.10) for the free fermion Green's functions and reordering the terms, we obtain
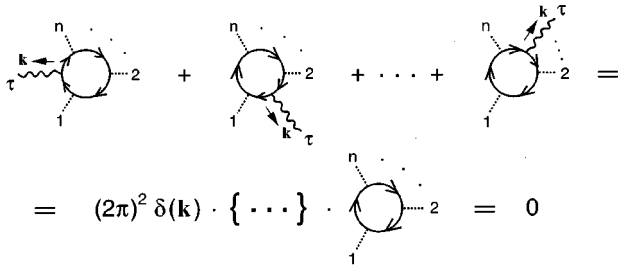
FIG. 8. Cancellation of a fermion loop with one 3 vertex with a wavy line and n further unspecified 3 vertices. The sum is taken over all permutations of the position of the wavy line, while the order of the remaining n vertices is kept fixed.

$$(2\pi)^2\delta(\mathbf{k})1\left\{[\theta(\tau-\tau')-n(\epsilon_0)]\hbar^{-1}\int_{\tau'}^{\tau}d\tau_2\Delta B(\tau_1-\tau_2)\right.$$

$$\left.-n(\epsilon_0)[1-n(\epsilon_0)]\hbar^{-1}\int_0^{\hbar\beta}d\tau_2\Delta B(\tau_1-\tau_2)\right\}$$

$$\times\exp[-\hbar^{-1}(\epsilon_0-\mu)(\tau-\tau')]. \tag{4.10}$$

Our assumption (4.2) implies that the second term in the curved brackets is zero. Parts of the first term can be combined again to the free fermion Green's function (2.10). Thus we obtain

$$(2\pi)^2\delta(\mathbf{k})\hbar^{-1}\int_{\tau'}^{\tau}d\tau_2\Delta B(\tau_1-\tau_2)G_0(\tau-\tau'), \tag{4.11}$$

which in terms of Feynman diagrams is exactly the right-hand side in Fig. 7, and the theorem is proven. We note that Theorem 1 (and the following theorems) is valid not only in our particular case where the motion of the electrons is restricted to the (degenerate) lowest Landau level. It can be proven in general for any free Green's function that can be represented in diagonal form by any (nondegenerate) single-particle states, where it is supposed that the 3 vertex is local in real space, which means that the interaction of the electrons is locally gauge invariant and the particle number is conserved.

Next we consider a closed fermion loop with n unspecified 3 vertices. We attach a wavy line to the loop via an additional 3 vertex and sum over all permutations of the position of the wavy line while the order of the other n vertices is kept fixed. In this way we obtain a sum of n diagrams, which is shown in Fig. 8 in the first line. Applying Theorem 1 we separate the wavy line as a factor and arrive at the second line in Fig. 8, while the expression in the curved brackets is given by

$$\{\cdots\}=\hbar^{-1}\int_{\tau_1}^{\tau_n}d\tau'\Delta B(\tau-\tau')+\hbar^{-1}\int_{\tau_2}^{\tau_1}d\tau'\Delta B(\tau-\tau')$$

$$+\cdots+\hbar^{-1}\int_{\tau_n}^{\tau_{n-1}}d\tau'\Delta B(\tau-\tau')$$

$$=0. \tag{4.12}$$

Thus, the sum of the diagrams cancels. By iteration this consideration can be extended straightforwardly to fermion
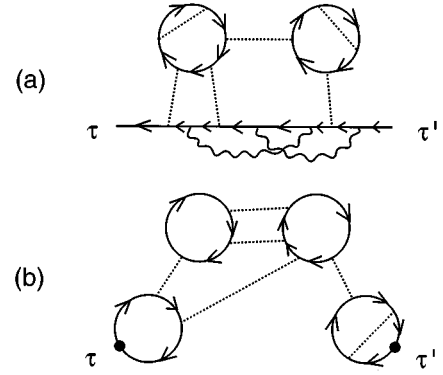

FIG. 9. Typical remaining diagrams of (a) the fermion Green's function $G(\tau-\tau')$ and (b) the connected density-density correlation function $\chi_{\rho\rho}(\mathbf{k},\tau-\tau')$ after application of Theorem 2. Wavy lines must be attached with both ends to an open fermion line and hence can be present only in diagrams of (a).

loops with more than one wavy line attached to it. In this way we arrive at the following theorem:

Theorem 2: Feynman diagrams that contain closed fermion loops with wavy lines (interactions ΔB) attached to them cancel due to the fact that the perturbation series sums over all permutations of the 3 vertices on each fermion loop.

As a consequence, in the remaining diagrams no wavy line is attached to closed fermion loops. This fact is shown in Fig. 9 for the diagrams of (a) the fermion Green's function $G(\tau-\tau')$ and (b) the connected density-density correlation function $\chi_{\rho\rho}(\mathbf{k},\tau-\tau')$. While the fermion lines can be connected by dotted interaction lines in any possible way, wavy lines, if they are present at all, must be attached to an *open* fermion line with *both ends*, as seen in Fig. 9(a). However, the diagrams of the density-density correlation function [Fig. 9(b)] contain only closed Fermion loops but no open fermion lines. Hence, in these diagrams the wavy lines drop out completely. In this way we obtain an easy result for the density-density correlation function. Let us denote by $\tilde{\chi}_{\rho\rho}(\mathbf{k},\tau-\tau')$ the connected density-density correlation function of an electron system where the electrons interact with the remaining interaction $\tilde{U}(\mathbf{k},\tau-\tau')$. The related Feynman diagrams contain only dotted interaction lines. Then, for the original density-density correlation function $\chi_{\rho\rho}(\mathbf{k},\tau-\tau')$ we obtain the relation

$$\chi_{\rho\rho}(\mathbf{k},\tau-\tau')=\tilde{\chi}_{\rho\rho}(\mathbf{k},\tau-\tau'), \tag{4.13}$$

order by order in perturbation theory by splitting the original interaction $U(\mathbf{k},\tau-\tau')$ (dashed line) as shown in Fig. 6 and applying Theorem 2 to the Feynman diagrams. Equation (4.13) is valid also for higher-order density correlation functions because the related Feynman diagrams contain only closed fermion loops. Thus, as an important result we find that a density correlation function of any order is not affected by the separation of a zero–wave-vector bosonic part of the interaction (a wavy line).

Now we continue with the fermion Green's function. To handle the diagrams with wavy lines on the open fermion line [Fig. 9(a)] we need further theorems. We consider an open fermion line with one end of a wavy line attached to it
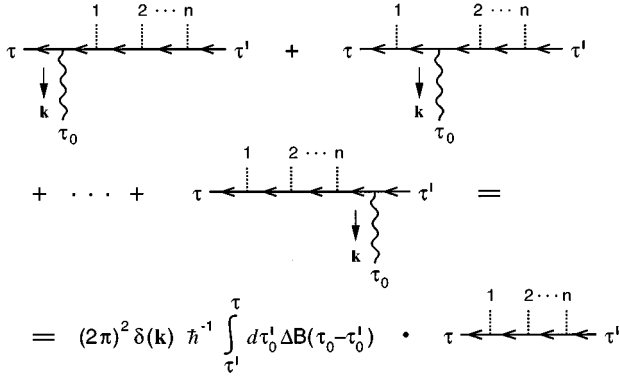
FIG. 10. Separation of a bosonic factor for an open fermion line with one end of a wavy line attached to it and n unspecified 3 vertices. The sum is taken over all permutations of the position of the wavy line, while the order of the remaining n vertices is fixed.

by a 3 vertex and n further unspecified vertices. We again sum over all permutations of the position of the wavy line and keep the order of the remaining vertices fixed. Applying Theorem 1 we separate a bosonic factor

$$(2\pi)^2\delta(\mathbf{k})\left\{\hbar^{-1}\int_{\tau_1}^{\tau}d\tau_0'\Delta B(\tau_0-\tau_0')\right.$$

$$+\hbar^{-1}\int_{\tau_2}^{\tau_1}d\tau_0'\Delta B(\tau_0-\tau_0')+\cdots$$

$$+\hbar^{-1}\int_{\tau_n}^{\tau_{n-1}}d\tau_0'\Delta B(\tau_0-\tau_0')$$

$$\left.+\hbar^{-1}\int_{\tau'}^{\tau_n}d\tau_0'\Delta B(\tau_0-\tau_0')\right\}$$

$$=(2\pi)^2\delta(\mathbf{k})\hbar^{-1}\int_{\tau'}^{\tau}d\tau_0'\Delta B(\tau_0-\tau_0') \quad (4.14)$$

and obtain the equation that is shown in Fig. 10. Next, we also attach the second end of the wavy line to the open fermion line and sum over all permutations of the positions of both ends, which lead to topologically nonequivalent diagrams. For the wavy line we must integrate over $\mathbf{k}$, so that the factor $(2\pi)^2\delta(\mathbf{k})$ disappears. Since the wavy line is not directed, its two ends are undistinguishable and we obtain an extra symmetry factor $1/2$. Thus, instead of (4.14) we then obtain the bosonic factor

$$\frac{1}{2}\hbar^{-2}\int_{\tau'}^{\tau}d\tau_0\int_{\tau'}^{\tau}d\tau_0'\Delta B(\tau_0-\tau_0')=\Delta\Phi(\tau-\tau'),$$
$$(4.15)$$

which can be identified with the function $\Delta\Phi(\tau-\tau')$ defined in (4.7). Further generalizations are straightforward. If we attach l wavy lines to the one open fermion line and sum over all topologically nonequivalent permutations of the ends of the wavy lines, we separate the bosonic factor

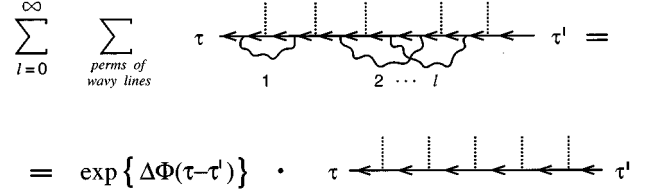$$\frac{1}{l!}[\Delta\Phi(\tau-\tau')]^l. \quad (4.16)$$

FIG. 11. Theorem 3: Exact treatment of the wavy lines that are connected with both ends to the open fermion line by separation of a bosonic exponential factor. The sum is taken over all permutations of the ends of the wavy lines, which lead to topologically non-equivalent diagrams. The order of the remaining vertices connected to dotted lines is kept fixed.

Here $1/l!$ is an additional symmetry factor that arises because the permutation of the l wavy lines leads to no new diagrams. Finally, we take the sum over the number of the wavy lines l and obtain an exponential function for the bosonic factor,

$$\sum_{l=0}^{\infty}\frac{1}{l!}[\Delta\Phi(\tau-\tau')]^l=\exp[\Delta\Phi(\tau-\tau')]. \quad (4.17)$$

Thus, we arrive at Theorem 3 which is stated diagrammatically in Fig. 11. Wavy lines that are attached to an open fermion line can be separated in terms of a bosonic factor that is exactly given by (4.17).

The remaining diagrams of the electron Green's function shown in Fig. 9(a) have exactly the form as the left-hand side of Theorem 3 in Fig. 11, where the unspecified vertices are connected to closed fermion loops by dotted lines. Thus, we can treat the wavy lines exactly by separating the exponential factor (4.17) while the second factor is a sum of Feynman diagrams that contain only dotted interaction lines but no wavy lines any more. Summing over all Feynman diagrams, for the original one-particle electron Green's function $G(\tau-\tau')$ we obtain the exact relation

$$G(\tau-\tau')=\exp[\Delta\Phi(\tau-\tau')]\tilde{G}(\tau-\tau'), \quad (4.18)$$

where $\Delta\Phi(\tau-\tau')$ is defined by (4.7) and $\tilde{G}(\tau-\tau')$ is a new Green's function of an electron system where the electrons interact via the remaining interaction $\tilde{U}(\mathbf{k},\tau-\tau')$ [above $\tilde{\chi}_{\rho\rho}(\mathbf{k},\tau-\tau')$ was defined analogously.] The Feynman diagrams of $\tilde{G}(\tau-\tau')$ are constructed only with dotted interaction lines. Since the exponential factor is a power series of the separated bosonic interaction part (wavy line), the right-hand side of (4.18) is a reordering of the perturbation series. Thus, for the electron Green's function we have found a formula that goes beyond perturbation theory. This formula (4.18) is a transformation formula for the electron Green's function with an important property: the occupation fraction of the lowest Landau level is not changed. Because of $\Delta\Phi(\tau=0)=0$, Eq. (4.18) implies

$$\nu=\tilde{\nu} \quad (4.19)$$

for $\nu=-G(\tau=-0)$ and $\tilde{\nu}=-\tilde{G}(\tau=-0)$. As a consequence, the neutralizing positive background charge density

ρ_b cancels the Hartree diagrams in both cases, in the perturbation series of $G(\tau-\tau')$ and in that of $\tilde{G}(\tau-\tau')$.

Our method can be applied also to higher-order Green's functions as, e.g., the two-particle Green's function. For each open fermion line we obtain an exponential factor (4.17) from the wavy lines connected with both ends to the same open fermion line. There will be also wavy lines that connect two different open fermion lines. From these wavy lines we obtain additional exponential factors, where the exponent is defined by a double integral similar to that in (4.7) but with four different imaginary times as integration boundaries. The resulting formulas for the higher-order Green's functions are similar to (4.18) but contain additional exponential factors.

V. OPTIMAL CHOICE OF THE BOSONIC INTERACTION PART: APPROXIMATE DERIVATION OF AN INDEPENDENT-BOSON MODEL

The main result of Sec. IV is the formula (4.18), which allows a factorization of the electronic Green's function $G(\tau-\tau')$ into an exactly known bosonic exponential factor and a new Green's function $\tilde{G}(\tau-\tau')$, which is given by a perturbation series in terms of the remaining interaction $\tilde{U}(\mathbf{k},\tau-\tau')$. Until now the bosonic function $B(\tau-\tau')$, which appears in the separation of the original interaction $U(\mathbf{k},\tau-\tau')$, is arbitrary and (4.18) is just an exact transformation formula for the electron Green's function. In Sec. III we have found that perturbation theory fails for the original Green's function $G(\tau-\tau')$, because the expected electronic spectral function $A(\epsilon)$ with a double-peak structure and a pseudogap at $\epsilon \approx \mu$ contradicts the results we have obtained by any feasible self-consistent approximation of the perturbation series. However, Eq. (4.18) enables us to transform the problem to the new Green's function $\tilde{G}(\tau-\tau')$. Our task is now to choose the bosonic function $B(\tau-\tau')$ in such a way that the new Green's function can be evaluated successfully by a perturbation series expansion. This means that the main nontrivial part of the spectral function $A(\epsilon)$, the double-peak structure, must be contained in the bosonic exponential factor, so that the spectral function $\tilde{A}(\epsilon)$ of the new Green's function has a *single peak* with a small width. The bosonic function $B(\tau-\tau')$ should be adjusted so that $\tilde{A}(\epsilon)$ is as close as possible to a delta function and $\tilde{G}(\tau-\tau')$ is as close as possible to a free Green's function.

Let us now consider the perturbation series of $\tilde{G}(\tau-\tau')$. We perform as many resummations as we can. Thus, we start with the self-consistent perturbation theory and express $\tilde{G}(\omega_n)$ via the Dyson equation,

$$\tilde{G}(\omega_n)=1/[-i\hbar\omega_n+\epsilon_0-\mu-\tilde{\Sigma}(\omega_n)], \qquad (5.1)$$

in terms of the self-energy $\tilde{\Sigma}(\omega_n)$, which can be written as a functional derivative,

$$\tilde{\Sigma}(\omega_n)=-\delta\tilde{\Phi}[\tilde{G}]/\delta\tilde{G}(\omega_n), \qquad (5.2)$$

where $\tilde{\Phi}[\tilde{G}]$ is a functional of the exact Green's function $\tilde{G}(\omega_n)$. The Feynman diagrams of $\tilde{\Sigma}(\tau-\tau')$ contain only thick propagator lines, which are identified with the exact Green's function $\tilde{G}(\tau-\tau')$ as it is shown in Fig. 12(a). The interaction $\tilde{U}(\mathbf{k},\tau-\tau')$ is represented by dotted lines in the
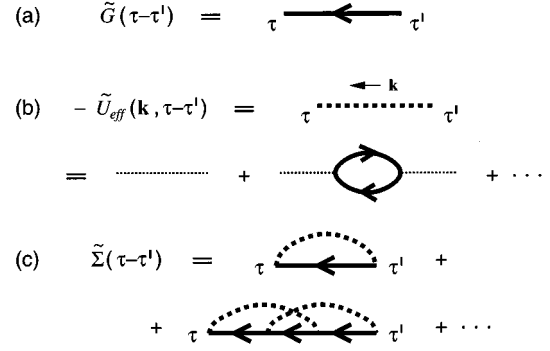

FIG. 12. (a) Exact Green's function $\tilde{G}(\tau-\tau')$ identified as thick propagator line, (b) summation of all interaction diagrams with polarization insertions leading to the effective interaction identified as thick dotted propagator line, and (c) perturbation series of the self-energy $\tilde{\Sigma}(\tau-\tau')$ up to second order in terms of irreducible diagrams with thick propagator lines and thick dotted interaction lines.

diagrams. A further resummation is possible with respect to polarization subdiagrams of the interaction. As shown in Fig. 12(b), we define the effective interaction $\tilde{U}_{\text{eff}}(\mathbf{k},\tau-\tau')$, associated with a thick dotted line, as the sum of all diagrams with two external dotted lines. In this way it is possible to express the self energy $\tilde{\Sigma}(\tau-\tau')$ in terms of irreducible diagrams that contain only thick propagator lines and thick dotted interaction lines. Up to second order in the effective interaction the Feynman diagrams of the self-energy are shown in Fig. 12(c). (One should have in mind that because of (4.19) the Hartree diagram is canceled by the neutralizing positively charged background.)

In a first-order approximation the self-energy is given by the first diagram in Fig. 12(c). Applying the Feynman rules of Sec. II we obtain the related analytical expression

$$\tilde{\Sigma}(\tau-\tau')=-\int\frac{d^2k}{(2\pi)^2}\tilde{U}_{\text{eff}}(\mathbf{k},\tau-\tau')$$
$$\times M(-\mathbf{k})\cdot\tilde{G}(\tau-\tau')\cdot M(\mathbf{k})$$
$$=-\int\frac{d^2k}{(2\pi)^2}\tilde{U}_{\text{eff}}(\mathbf{k},\tau-\tau')$$
$$\times\exp[-\tfrac{1}{2}\mathbf{k}^2\ell^2]\tilde{G}(\tau-\tau'), \qquad (5.3)$$

where in the second line we have used the algebraic formulas (2.13). Considering the Feynman diagrams of the perturbation series in Fig. 12(b) carefully, we can express the effective interaction $\tilde{U}_{\text{eff}}(\mathbf{k},\tau-\tau')$ exactly in terms of the bare interaction $\tilde{U}(\mathbf{k},\tau-\tau')$ and the connected density-density correlation function $\tilde{\chi}_{\rho\rho}(\mathbf{k},\tau-\tau')$ by

$$\tilde{U}_{\text{eff}}(\mathbf{k},\tau-\tau')=\tilde{U}(\mathbf{k},\tau-\tau')-\hbar^{-2}\int_0^{\hbar\beta}d\tau_1\int_0^{\hbar\beta}d\tau_2$$
$$\times\tilde{U}(\mathbf{k},\tau-\tau_1)\tilde{\chi}_{\rho\rho}(\mathbf{k},\tau_1-\tau_2)\tilde{U}(\mathbf{k},\tau_2-\tau').$$
$$(5.4)$$

Now, on the right-hand side we want to replace the quantities with a tilde by quantities without a tilde. In the second term

we can just omit the tilde for the following reasons. In Sec. IV we have shown by (4.13) that the density-density correlation functions with a tilde and without a tilde are equal. The two interactions in the second term of (5.4) are represented by two external dotted lines in the Feynman diagrams [Fig. 12(b)], which are always connected with one end to closed Fermion loops. Thus, applying Theorem 2 together with the equation in Fig. 6(a) we can just replace the two external dotted lines by dashed lines. Hence, we may omit the tilde also on the interactions in the second term of (5.4). For the first term we use the equation in Fig. 6(b) and (4.3). We remember that the original interaction $U(\mathbf{k}, \tau - \tau')$ is instantaneous and expressed in terms of the Coulomb potential $V(\mathbf{k})$ by (2.11). Taking everything together, we then arrive at the following formula for the effective interaction:

$$\tilde{U}_{\mathrm{eff}}(\mathbf{k}, \tau - \tau') = V(\mathbf{k}) \sum_n \hbar \delta(\tau - \tau' + n \hbar \beta) + (2\pi)^2 \delta(\mathbf{k})$$

$$\times \left[B(\tau - \tau') - 2\Delta \sum_n \hbar \delta(\tau - \tau' + n \hbar \beta) \right]$$

$$- V(\mathbf{k}) \chi_{\rho\rho}(\mathbf{k}, \tau - \tau') V(\mathbf{k}). \quad (5.5)$$

Next we insert the effective interaction (5.5) into the self-energy (5.3) and obtain

$$\tilde{\Sigma}(\tau - \tau') = - \int \frac{d^2 k}{(2\pi)^2} V(\mathbf{k}) \exp[-\tfrac{1}{2} \mathbf{k}^2 \ell^2]$$

$$\times \tilde{G}(\tau - \tau') \sum_n \hbar \delta(\tau - \tau' + n \hbar \beta)$$

$$+ 2\Delta \ \tilde{G}(\tau - \tau') \sum_n \hbar \delta(\tau - \tau' + n \hbar \beta)$$

$$- B(\tau - \tau') \tilde{G}(\tau - \tau')$$

$$+ \int \frac{d^2 k}{(2\pi)^2} \chi_{\rho\rho}(\mathbf{k}, \tau - \tau') [V(\mathbf{k})]^2$$

$$\times \exp[-\tfrac{1}{2} \mathbf{k}^2 \ell^2] \tilde{G}(\tau - \tau') \quad (5.5)$$

The first two terms are instantaneous in the imaginary times because of the delta functions. Thus, in these terms we can replace $\tilde{G}(\tau - \tau') \rightarrow \tilde{G}(0)$. However, since the Green's function $\tilde{G}(\tau - \tau')$ has a jump at $\tau - \tau' = 0$, we must be careful. The first term in (5.6) is the Fock self-energy. To take the normal ordering of the fermion operators in the Hamiltonian (2.1) into account, we must choose the value $\tilde{G}(-0) = -\tilde{\nu} = -\nu$. The second term arises from the independent bosons. Since the wavy lines are not directed and the bosonic functions are symmetric, we must choose the symmetric value $(1/2)[\tilde{G}(+0) + \tilde{G}(-0)] = (1/2)(1 - 2\tilde{\nu}) = (1/2)(1 - 2\nu)$ in that term. The last two terms are nontrivially imaginary-time dependent and contain retardation effects. They cancel if we choose the bosonic function

$$B(\tau - \tau') = \int \frac{d^2 k}{(2\pi)^2} \chi_{\rho\rho}(\mathbf{k}, \tau - \tau') [V(\mathbf{k})]^2 \exp[-\tfrac{1}{2} \mathbf{k}^2 \ell^2]. \quad (5.7)$$

Thus, we end up with an instantaneous self-energy,

$$\tilde{\Sigma}(\tau - \tau') = \left[\nu \int \frac{d^2 k}{(2\pi)^2} V(\mathbf{k}) \exp[-\tfrac{1}{2} \mathbf{k}^2 \ell^2] - (2\nu - 1)\Delta \right] \sum_n \hbar \delta(\tau - \tau' + n \hbar \beta), \quad (5.8)$$

which after a Fourier transformation becomes a constant,

$$\tilde{\Sigma}(\omega_n) = \nu \int \frac{d^2 k}{(2\pi)^2} V(\mathbf{k}) \exp[-\tfrac{1}{2} \mathbf{k}^2 \ell^2] - (2\nu - 1)\Delta. \quad (5.9)$$

We insert this result of our first-order approximation into the Dyson equation (5.1) and obtain the Green's function

$$\tilde{G}(\omega_n) = 1/[-i\hbar \omega_n + \epsilon_1 - \mu], \quad (5.10)$$

which after a Fourier back transformation becomes

$$\tilde{G}(\tau - \tau') = [\theta(\tau - \tau') - n(\epsilon_1)] \exp[-\hbar^{-1}(\epsilon_1 - \mu)(\tau - \tau')] \quad (5.11)$$

in imaginary-time representation. Here

$$\epsilon_1 = \epsilon_0 - \nu \int \frac{d^2 k}{(2\pi)^2} V(\mathbf{k}) \exp[-\tfrac{1}{2} \mathbf{k}^2 \ell^2] + (2\nu - 1)\Delta \quad (5.12)$$

is the renormalized energy and $n(\epsilon_1)$ is the related value of the Fermi distribution function. From (5.10) and (5.11) it is clearly seen that in our first-order approximation together with the bosonic function (5.7) we obtain a *free* Green's function for $\tilde{G}(\tau - \tau')$ with a shifted energy (5.12). There are two contributions of the energy shift. The first one is the Fock energy. The second one originates from the independent bosons and is represented by Δ. (The Hartree energy is canceled by the neutralizing background.) For the related spectral function $\tilde{A}(\epsilon)$ we obtain a delta function,

$$\tilde{A}(\epsilon) = \delta(\epsilon - \epsilon_1). \quad (5.13)$$

Thus, in our approximation, where we take only the first diagram of the self-energy shown in Fig. 12(c) into account, we have reached our goal as well as possible with the choice (5.7) for the bosonic function $B(\tau - \tau')$. The spectral function $\tilde{A}(\epsilon)$ is a delta function, and $\tilde{G}(\tau - \tau')$ is a free Green's function with shifted energy.

Now, from (4.18) and (5.11) we obtain the electron Green's function

$$G(\tau - \tau') = [\theta(\tau - \tau') - n(\epsilon_1)] \exp[-\hbar^{-1}(\epsilon_1 - \mu)(\tau - \tau') + \Delta \Phi(\tau - \tau')] \quad (5.14)$$

where $\Delta \Phi(\tau - \tau')$ is defined by (4.8) together with the bosonic function (5.7). This result has exactly the form of the solution of the independent-boson model.[6] In this model the function $B(\tau - \tau')$ is the integral of the independent-boson Green's function weighted by the square of the electron-boson interaction. If here one interprets $\chi_{\rho\rho}(\mathbf{k}, \tau - \tau')$ as the independent-boson Green's function and the Coulomb potential $V(\mathbf{k})$ as the electron-boson interaction, then $B(\tau - \tau')$ in (5.7) has exactly this form, where the exponential factor is an additional weight factor arising from the projection to the lowest Landau level. Thus, we can identify and interpret the

collective excitations described by the density-density correlation function $\chi_{\rho\rho}(\mathbf{k}, \tau - \tau')$ as the *independent bosons*. However, there is one difference. While in the independent-boson model the bosons are assumed to be free, here the collective excitations have *finite lifetimes* because the spectral function $\chi_{\rho\rho}''(\mathbf{k}, \epsilon)$ consists of peaks with finite widths.

It is straightforward and easy to find a Hamiltonian of an independent-boson model which has the Green's function (5.14) as its solution. In this way we can say that with our transformation formula (4.18) and our first-order approximation for $\tilde{G}(\tau - \tau')$ we have found a systematic way of deriving approximately an independent-boson model from the microscopic quantum-field theory of the interacting electron system. Johansson and Kinaret[5] have started directly with an independent-boson model to explain the tunneling experiments.[1-3] While the electronic part of their model is quite similar to our result, they use magnetophonons of a Wigner crystal as an approximation for the collective excitations in the strongly correlated electron liquid. There are some differences. However, our method mainly supports the approach of Johansson and Kinaret on a microscopic level.

The independent-boson model is a very intuitive way to explain the tunneling experiments[1-3] and can be viewed as a quantitative realization of the qualitative ideas reported already in the first paper on this experiment by Eisenstein *et al.*[1] However, this model is an approximation of the real physical problem. Thus, one has to find out how good this approximation is. Our method is based on a perturbation series expansion of the transformed Green's function $\tilde{G}(\tau - \tau')$, so that we should consider the higher-order Feynman diagrams of the self-energy $\tilde{\Sigma}(\tau - \tau')$ in Fig. 12(c). First of all, if we would apply our method to the original independent-boson model with only one fermion state,[6] then all higher-order diagrams would cancel exactly. However, in the present case we have many electrons in the degenerate lowest Landau level so that the higher-order diagrams are nonzero. To get a feeling of the quality of the approximation one should consider the second-order diagram in Fig. 12(c). In the effective interaction (5.5) (the thick dotted line) the bosonic function $B(\tau - \tau')$ defined by (5.7) provides that the term related to the collective excitations (the last term) is canceled at least partially if the integral over $\mathbf{k}$ is taken. How perfect this cancellation is depends on the exponential weight factor, which arises from the algebraic formula (2.13a) for the matrix elements of the 3 vertices. In the first-order diagram of the self-energy in Fig. 12(c) the cancellation is complete by the choice (5.7). However, in the higher-order diagrams the $\mathbf{k}$-dependent exponential factors depend sensitively on the topology of the diagrams. Hence, the second-order diagram yields a contribution to the self-energy which contains nontrivial time-dependent and retardation effects. This contribution should be small so that in the second-order approximation $\tilde{G}(\tau - \tau')$ differs not too much from the free Green's function and the related spectral function $\tilde{A}(\epsilon)$ is a *single peak* with a relatively small width.

We have not proven explicitly if the noninstantaneous contributions of the self-energy due to the higher-order diagrams are really small. It is not clear if these contributions are small at all. In principle one can improve our approach to higher orders by constructing a perturbation series for the

bosonic function $B(\tau - \tau')$ in such a way that the noninstantaneous terms of the self-energy are canceled order by order. We believe that our approach is good at least to some extent, because it provides a simple and intuitive explanation of the effect and because it yields quantitative results for the tunneling current $I(V)$ which agree with the experiments quite well (see Sec. VI).

Once we believe that our theory is reasonable, we can calculate the electron Green's function $G(\tau - \tau')$ by Eqs. (5.14), (4.8), and (5.7) if the density-density correlation function $\chi_{\rho\rho}(\mathbf{k}, \tau - \tau')$ is known. The occupation fraction of the lowest Landau level

$$\nu = -G(\tau - \tau' = -0) = n(\epsilon_1) \qquad (5.15)$$

is simply given by the Fermi distribution function with the renormalized energy (5.12) as the argument. It turns out that our result for $\nu(\mu)$ is a continuous function of the chemical potential μ. Thus, our theory does not include the subtleties of the fractional quantum Hall effect (FQHE) as, e.g., steps and plateaus in $\nu(\mu)$. However, in the tunneling experiments[1-3] the FQHE seems to play a minor role, so that this deficiency of our theory is not very important. Inserting (5.14) into (3.5) we obtain the particle-hole pair propagator

$$\chi(\tau - \tau') = \nu(1 - \nu)\exp[2\Delta\Phi(\tau - \tau')], \qquad (5.16)$$

which does not depend explicitly on the renormalized energy (5.12). Then from the Fourier transforms $G(\omega_n)$ and $\chi(\Omega_n)$ we determine the spectral functions $A(\epsilon)$ and $\chi''(\epsilon)$ by analytic continuations to real frequencies via Padé approximation. Finally, from (3.6) we obtain $I(V)$. In a recent paper about moments of the spectral functions[9] it was pointed out that a measure of the tunneling pseudogap can be obtained from a sum rule of the current-voltage characteristic $I(V)$. Thus, from (3.6), (5.16), and (4.8) we can calculate this sum-rule gap and obtain

$$e \int_0^\infty dV\, V\, I(V) \bigg/ \int_0^\infty dV\, I(V)$$

$$= \int_0^\infty d\epsilon\, \epsilon\, \chi''(\epsilon) \bigg/ \int_0^\infty d\epsilon\, \chi''(\epsilon)$$

$$= -\hbar \frac{\partial}{\partial\tau}\chi(\tau)\big|_{\tau = +0} \big/ \chi(\tau = 0)$$

$$= -2\hbar \frac{\partial}{\partial\tau}\Delta\Phi(\tau)\big|_{\tau = +0} = 2\Delta. \qquad (5.17)$$

Since the current $I(V)$ in (1.1) is a convolution of electronic spectral functions, this sum-rule gap is related to the pseudogap of $A(\epsilon)$. If $A(\epsilon)$ has a double-peak structure as expected, then 2Δ is approximately the energy difference of the positions of the two peaks. Hence, Δ is an important parameter in our theory. Inserting (5.7) into (4.4) we obtain

$$\Delta = \frac{1}{2}\int \frac{d^2k}{(2\pi)^2}\chi_{\rho\rho}(\mathbf{k}, \Omega_n = 0)[V(\mathbf{k})]^2\exp[-\tfrac{1}{2}\mathbf{k}^2 \ell^2].$$

$$(5.18)$$

Here $\chi_{\rho\rho}(\mathbf{k}, \Omega_n = 0)$ is the thermodynamic susceptibility that describes the linear response of the electron density on an

applied external potential in thermal equilibrium. Thus, the quantity Δ in (5.18) can be interpreted as minus the change of the energy (the thermodynamic potential) of the electron system due to relaxation in an applied external potential $V(\mathbf{r})$ up to second order. The origin of this external potential is the tunneling of an electron. If one electron tunnels into the two-dimensional layer, it then creates a Coulomb potential $V(\mathbf{r}) = e^2/|\mathbf{r}|$ in its surrounding, which causes a relaxation and a change of the electron density and hence a reduction of the electrostatic correlation energy given by (5.18). The exponential factor arises due to the fact that this additional electron must satisfy the Pauli exclusion principle with the remaining electrons. [In the Fock energy, the second term in (5.12), the exponential factor appears for the same reason.]

Thus, on a rough scale, from our theory we can read off a qualitative explanation for the effect which is similar to that of Eisenstein et $al.$[1] and of Johansson and Kinaret.[5] An electron that tunnels $into$ the layer needs an additional energy Δ to compensate the correlation energy before the system can relax. In some sense one can say that the electron tunnels into an interstitial place. Hence, the $electron$ $peak$ of the spectral function $A_+(\epsilon)$ is shifted to higher energies by Δ. An electron that tunnels out of the layer leaves a hole which has a correlation energy $-\Delta$ because of its opposite charge. Hence, the $hole$ $peak$ of the spectral function $A_-(\epsilon)$ is shifted to lower energies by $-\Delta$. As a result, the electronic spectral function $A(\epsilon) = A_+(\epsilon) + A_-(\epsilon)$ has two peaks, whose positions are separated approximately by 2Δ. Since the system relaxes into equilibrium within a certain time after the tunneling process, the two peaks have finite widths, which are determined by the explicit form of the spectrum $\chi_{\rho\rho}(\mathbf{k},\epsilon)$ of the collective excitations. If the relaxation process is slow, then the two peaks will be well established. Otherwise, in the case of a quick relaxation the two peaks will melt together into one peak.

Our theory yields a formula for the electron Green's function $G(\tau - \tau')$ which needs the density-density correlation function $\chi_{\rho\rho}(\mathbf{k},\tau - \tau')$ as an input. In principle, one can calculate $\chi_{\rho\rho}(\mathbf{k},\tau - \tau')$ by perturbation theory, e.g., in an RPA approximation. The result, however, is not very accurate. In any approximation one must be very careful that $\chi_{\rho\rho}(\mathbf{k},\tau - \tau')$ has the right hydrodynamic behavior for small $\mathbf{k}$ and small frequencies, imposed by the particle conservation. Explicitly this means $\chi_{\rho\rho}(\mathbf{k}=\mathbf{0},\tau - \tau') = constant$, so that the assumptions of the theorems in Sec. IV are satisfied and that the transition from the effective potential (5.4) to the formula (5.5) is valid. We have found that the density-density correlation function calculated by a $self$-$consistent$ RPA approximation (as in Sec. III) violates this property and thus is not successful. [The result is an electronic spectral function $A(\epsilon)$ with a single peak that looks similar to the result of Sec. III in Fig. 3.] In Sec. IV we have proven the equality $\chi_{\rho\rho}(\mathbf{k},\tau - \tau') = \tilde{\chi}_{\rho\rho}(\mathbf{k},\tau - \tau')$ order by order in perturbation theory. This implies that by our method we do not obtain a formula for the density-density correlation function that goes beyond perturbation theory.

The quantum-field theory does not yield a reliable result for the density-density correlation function. Nevertheless, it is instructive to do the standard RPA calculation, because it yields a simple result and some feeling for the order of mag-

nitudes (and it does not violate the assumptions of the theorems). From the free-electron Green's function (2.10) we obtain the free pair propagator $\chi_0(\Omega_n) = \beta\nu(1-\nu)\delta_{\Omega_n,0}$ and hence the RPA density-density correlation function

$$\chi_{\rho\rho}(\mathbf{k},\Omega_n) = \frac{\beta\nu(1-\nu)}{1 + \lambda(\mathbf{k})\beta\nu(1-\nu)}\delta_{\Omega_n,0}, \qquad (5.19)$$

where $\lambda(\mathbf{k}) = (2\pi\ell^2)^{-1}\exp\{-(1/2)\mathbf{k}^2\ell^2\}V(\mathbf{k})$ is the effective interaction. The related spectrum $\chi_{\rho\rho}''(\mathbf{k},\epsilon)$ has its weight at $zero$ $energy$, so that the present approximation is somewhat oversimplified. We can now proceed with Eqs. (5.7), (4.8), and (5.14) to calculate the electron Green's function. Because of the simplicity of (5.19) all integrals can be evaluated exactly, and we obtain

$$\Delta\Phi(\tau - \tau') = -\hbar^{-1}\Delta|\tau - \tau'| + \hbar^{-2}(k_B T\Delta)(\tau - \tau')^2, \qquad (5.20)$$

where

$$\Delta = \pi\ell^2 \int \frac{d^2k}{(2\pi)^2} \frac{[\lambda(\mathbf{k})]^2\beta\nu(1-\nu)}{1 + \lambda(\mathbf{k})\beta\nu(1-\nu)} \qquad (5.21)$$

and $\beta = 1/k_B T$. The analytic continuation to real times (Keldysh formalism) can be done easily. Substituting $\tau \to \pm 0 + it$ in the Green's function (5.14) we obtain the real-time Green's functions $G_+(t)$ and $G_-(t)$, the Fourier transforms of which are the spectral functions

$$A_+(\epsilon) = (1-\nu)[2\pi\delta]^{-1/2}\exp[-(\epsilon - [\epsilon_1 + \Delta])^2/2\delta^2], \qquad (5.22a)$$

$$A_-(\epsilon) = \nu[2\pi\delta]^{-1/2}\exp[-(\epsilon - [\epsilon_1 - \Delta])^2/2\delta^2], \qquad (5.22b)$$

where $\delta = (2k_B T\Delta)^{1/2}$. Thus, we obtain an electronic spectral function $A(\epsilon) = A_+(\epsilon) + A_-(\epsilon)$, which consists of two Gaussian peaks of width δ the positions of which are separated by the sum-rule gap 2Δ. At low temperatures $T \ll \Delta/k_B$ the width is quite small, $\delta \ll 2\Delta$, so that $A(\epsilon)$ has a well-established double-peak structure. However, in the zero-temperature limit $T \to 0$ the peaks become δ functions because of $\delta = (2k_B T\Delta)^{1/2} \to 0$ while the sum-rule gap $2\Delta \to (\pi/2)e^2/\ell$ becomes the Fock energy. This zero-temperature result is artificial and arises from the fact that we have assumed a spectrum of zero-energy collective excitations. According to the experiments, $A(\epsilon)$ must have two broad peaks also for $T = 0$. Thus, in a more profound theory we need a more realistic spectrum $\chi_{\rho\rho}''(\mathbf{k},\epsilon)$ of the collective excitations.

Since the input of the independent-boson model is the $\mathbf{k}$ integral (5.7), the $\mathbf{k}$ dependence of the spectrum of the collective excitations is not so important. More precisely, the electron Green's function $G(\tau - \tau')$ and the electronic spectral function $A(\epsilon)$ depend only on the integrated spectral function

$$B''(\epsilon) = \int \frac{d^2k}{(2\pi)^2}\chi_{\rho\rho}''(\mathbf{k},\epsilon)[V(\mathbf{k})]^2\exp[-\tfrac{1}{2}\mathbf{k}^2\ell^2]. \qquad (5.23)$$

Thus, we can play around with the independent-boson model to find out what $B''(\epsilon)$ must qualitatively look like so that the

resulting $A(\epsilon)$ fits the experiments. It turns out that the form of $A(\epsilon)$ is determined mainly by the *energy* of the collective excitations, i.e., the energy at which $B''(\epsilon)$ has its main spectral weight, while the precise form of $B''(\epsilon)$ is not so important. We find that high-energy collective excitations produce a single peak for $A(\epsilon)$, while collective excitations with low energies $\epsilon \lesssim 0.3\Delta$ yield a double-peak structure for low temperatures. The electronic spectral function $A(\epsilon)$ with two broad peaks at low temperatures, as expected from the experiments, is obtained if $B''(\epsilon)$ has its main spectral weight in the interval $0 < |\epsilon| \lesssim 0.2\Delta$ where $2\Delta \sim e^2/\ell$. In the next section we determine $B''(\epsilon)$ by the single-mode approximation[13] and then calculate $A(\epsilon)$, $\chi''(\epsilon)$, and $I(V)$.

VI. SINGLE-MODE APPROXIMATION FOR THE COLLECTIVE EXCITATIONS

In a simple approximation we can assume that for a given wave vector $\mathbf{k}$ density waves approximately are collective modes with a single energy $E(\mathbf{k})$ and an infinite lifetime. This means that for the spectral function of the collective excitations we make the ansatz

$$\chi''_{\rho\rho}(\mathbf{k},\epsilon) = a(\mathbf{k})[\delta(\epsilon - E(\mathbf{k})) - \delta(\epsilon + E(\mathbf{k}))], \quad (6.1)$$

which is called single-mode approximation. The energy $E(\mathbf{k})$ and the spectral weight $a(\mathbf{k})$ are determined by sum rules for $\chi''_{\rho\rho}(\mathbf{k},\epsilon)$ and can be calculated according to the magnetoroton theory of collective excitations developed by Girvin, MacDonald, and Platzman.[13] In this theory all quantities can be expressed in terms of the static structure factor $\bar{S}(\mathbf{k})$, which is defined as the Fourier transform of the static correlation function of the density $\hat{\rho}(\mathbf{r}) = \hat{\psi}^+(\mathbf{r})\hat{\psi}(\mathbf{r})$ *projected to the lowest Landau level*,

$$\langle \hat{\rho}(\mathbf{r})\hat{\rho}(\mathbf{r}') \rangle = \int \frac{d^2k}{(2\pi)^2} e^{i\mathbf{k}(\mathbf{r}-\mathbf{r}')} \rho_0 \bar{S}(\mathbf{k}). \quad (6.2)$$

Here the uniform particle density of the system $\rho_0 = \nu/2\pi\ell^2$ appears for convention of the normalization of the static structure factor. Now, one can straightforwardly prove the sum rule

$$\frac{1}{2} \int d\epsilon \, \coth[\beta\epsilon/2] \chi''_{\rho\rho}(\mathbf{k},\epsilon) = \chi_{\rho\rho}(\mathbf{k},\tau=0) = \rho_0 \bar{S}(\mathbf{k}) \quad (6.3)$$

using the property that $\chi''_{\rho\rho}(\mathbf{k},\epsilon)$ is antisymmetric in ϵ. The factor $\coth[\beta\epsilon/2]$ is related to a fluctuation-dissipation theorem which connects the dynamic susceptibility $\chi''_{\rho\rho}(\mathbf{k},\epsilon)$ with the dynamic structure factor. In a similar way a second sum rule can be proven,

$$\frac{1}{2} \int d\epsilon \, \epsilon \chi''_{\rho\rho}(\mathbf{k},\epsilon) = \frac{1}{2} \left(\left[-\frac{1}{\hbar} \frac{\partial}{\partial\tau} \chi_{\rho\rho}(\mathbf{k},\tau) \right] \Big|_{\tau=+0} \right.$$
$$\left. - \left[-\frac{1}{\hbar} \frac{\partial}{\partial\tau} \chi_{\rho\rho}(\mathbf{k},\tau) \right] \Big|_{\tau=-0} \right)$$
$$= \rho_0 \bar{f}(\mathbf{k}), \quad (6.4)$$

where $\bar{f}(\mathbf{k})$ is the oscillator strength defined by the Fourier transform of the double commutator

$$\frac{1}{2} \langle [[\hat{\rho}(\mathbf{r}),\hat{K}],\hat{\rho}(\mathbf{r}')] \rangle = \int \frac{d^2k}{(2\pi)^2} e^{i\mathbf{k}(\mathbf{r}-\mathbf{r}')} \rho_0 \bar{f}(\mathbf{k}). \quad (6.5)$$

Here $\hat{K} = \hat{H} - \mu\hat{N}$ is an operator related to the Hamiltonian $\hat{H}$ (2.1), of the system and the operator of the total particle number $\hat{N}$. Inserting the single-mode approximation (6.1) for the spectral function $\chi''_{\rho\rho}(\mathbf{k},\epsilon)$ into the sum rules (6.3) and (6.4), the energy integrals on the left-hand sides can be evaluated trivially, and we obtain the formulas

$$a(\mathbf{k}) = \rho_0 \bar{S}(\mathbf{k}) \tanh[\beta E(\mathbf{k})/2], \quad (6.6)$$

$$E(\mathbf{k}) = \rho_0 \bar{f}(\mathbf{k})/a(\mathbf{k}). \quad (6.7)$$

Because of the factor $\tanh[\beta E(\mathbf{k})/2]$ these equations are the generalizations of the formula of the single-mode energy in Ref. 13 to finite temperatures [compare with (4.19) in the second paper of Ref. 13 and note that for $\bar{S}(\mathbf{k})$ and $\bar{f}(\mathbf{k})$ we use the same notation while our $E(\mathbf{k})$ must be identified with $\Delta(\mathbf{k})$ in this paper]. Thus, if $\bar{S}(\mathbf{k})$ and $\bar{f}(\mathbf{k})$ are known, with these formulas we can calculate $a(\mathbf{k}), E(\mathbf{k})$ and then obtain the spectral functions $\chi''_{\rho\rho}(\mathbf{k},\epsilon)$ and $B''(\epsilon)$ via (6.1) and (5.23). Equivalent to (6.1) are the equations

$$\chi_{\rho\rho}(\mathbf{k},\tau) = a(\mathbf{k})(\{\theta(\tau) + n_B[E(\mathbf{k})]\}\exp[-\hbar^{-1}E(\mathbf{k})\tau]$$
$$+ \{\theta(-\tau) + n_B[E(\mathbf{k})]\}\exp[+\hbar^{-1}E(\mathbf{k})\tau]), \quad (6.8)$$

$$\chi_{\rho\rho}(\mathbf{k},\Omega_n) = a(\mathbf{k})2E(\mathbf{k})/\{(\hbar\Omega_n)^2 + [E(\mathbf{k})]^2\} \quad (6.9)$$

in imaginary-time representation and Matsubara representation, respectively, where $n_B(\epsilon) = 1/[e^{\beta\epsilon} - 1]$ is the Bose distribution function. From (6.8) and (5.7) we obtain the bosonic function $B(\tau)$, which we need as an input to calculate the function $\Delta\Phi(\tau - \tau')$ by (4.8) and finally the fermion Green's function $G(\tau - \tau')$ by (5.14).

Girvin, MacDonald, and Platzman[13] have evaluated the double commutator on the left-hand side of (6.5) and shown that for densities projected to the lowest Landau level the oscillator strength $\bar{f}(\mathbf{k})$ can be expressed *exactly* in terms of the structure factor $\bar{S}(\mathbf{k})$. The resulting formula is given by (4.15) in the second paper of Ref. 13. We replace the exponential functions with imaginary arguments by sine and cosine functions and transform the momentum integration to polar coordinates. Then we write the formula in the form

$$\bar{f}(k) = \frac{1}{2}(2\pi)^{-2} \int_0^\infty q\,dq \int_0^{2\pi} d\varphi V(q)(2\sin[\tfrac{1}{2}qk\ell^2\sin\varphi])^2$$
$$\times [-\bar{S}(q)e^{-k^2\ell^2/2}$$
$$+ \bar{S}(\sqrt{k^2 + q^2 + 2kq\cos\varphi})e^{kq\cos\varphi}], \quad (6.10)$$

which is convenient for numerical evaluation. Here $V(q) = 2\pi e^2/q$ is the two-dimensional Fourier transform of the Coulomb interaction potential. Because of the isotropy of the liquid state the structure factor and all other quantities depend only on the absolute value $k = |\mathbf{k}|$ but not on the direction of the wave vector. Thus, from now on we write k instead of $\mathbf{k}$ in the arguments of the functions. We perform

first the integral over the angle φ and then the integral over the radial wave number q. All functions are sufficiently smooth so that the numerical integrations cause no problems and are accurate.

Now, all we need to evaluate the quantities $a(k)$, $E(k)$, and the spectral function (6.1) is the static structure factor $\bar{S}(k)$. Girvin, MacDonald, and Platzman[13] calculated the structure factor for fractional quantum Hall ground states with occupation fractions $\nu=1/3$, $1/5$, and some others by two different methods, a Monte Carlo and a hypernetted-chain calculation. Qualitatively $\bar{S}(k)$ has the following form: for $k\rightarrow 0$ and $k\rightarrow\infty$ it is zero, and for wave numbers around $k\approx\ell^{-1}$ it has a single maximum. Since we need $\bar{S}(k)$ for all occupation fractions ν in the interval $0<\nu<1$, mainly close to $\nu=1/2$, we should establish an easy interpolation formula. However, it turns out that the mode energy $E(k)$ is very sensitive on small details of $\bar{S}(k)$. Thus, we must be very careful in choosing an appropriate ansatz for $\bar{S}(k)$.

According to Girvin, MacDonald, and Platzman[13] we start with the pair-correlation function $g(r)$ of the "liquid" ground state, which can be expanded in terms of lowest-Landau-level eigenfunctions with angular momentum m for the relative motion as

$$g(r)=1-e^{-r^2/2\ell^2}+\sum_{\substack{m=1\\ \text{odd}}}^{\infty} c_m \frac{2}{m!}\left(\frac{r^2}{4\ell^2}\right)^m e^{-r^2/4\ell^2}.$$
(6.11)

Here the c_m with odd $m=1,3,5,\ldots$ are coefficients which represent the nontrivial correlations of the electronic ground state in the fractional quantum Hall regime. For a free electron gas it is $c_m=0$ for all m. Positive definiteness requires $c_m\geq -1$ for all m. For a correlated state the c_m are nonzero but satisfy the limiting behavior $c_m\rightarrow 0$ for $m\rightarrow\infty$. By Fourier transformation and projection to the lowest Landau level we find an equivalent expansion for the structure factor which reads

$$\bar{S}(k)=(1-\nu)e^{-k^2\ell^2/2}+4\nu\sum_{\substack{m=1\\ \text{odd}}}^{\infty} c_m L_m(k^2\ell^2)e^{-k^2\ell^2},$$
(6.12)

where $L_m(z)$ are the Laguerre polynomials. Now, our strategy is to find a good interpolation formula for $\bar{S}(k)$ with only a few nonzero c_m. It turns out that charge neutrality and perfect screening sum rules imply two restrictions on the coefficients c_m, which read[13]

$$\sum_{\substack{m=1\\ \text{odd}}}^{\infty} c_m = -\tfrac{1}{4}(1-\nu)/\nu,$$
(6.13)

$$\sum_{\substack{m=1\\ \text{odd}}}^{\infty} (m+1)c_m = -\tfrac{1}{8}(1-\nu)/\nu.$$
(6.14)

Expanding $\bar{S}(k)$ for small k in powers of k^2, the two restrictions imply that the terms proportional to k^0 and k^2 vanish. Thus, for small k up to leading order we have

$$\bar{S}(k)=(1-\nu)\tfrac{1}{2}\gamma(k^2\ell^2)^2+\cdots,$$
(6.15)

where γ is a parameter which is positive and depends in a particle-hole symmetric way on ν. It turns out that the mode energies $E(k)$ depend sensitively on γ for small k. Thus, we must consider γ as an important parameter and choose it appropriately. Expanding (6.12) with respect to k up to fourth order and comparing with (6.15) we obtain a third equation for the coefficients c_m given by

$$\frac{1}{4}+\frac{2\nu}{1-\nu}\sum_{\substack{m=1\\ \text{odd}}}^{\infty}(m+1)(m+2)c_m = \gamma.$$
(6.16)

For simplicity we assume that only the first three coefficients c_1, c_3, and c_5 are nonzero while $c_m=0$ for $m\geq 7$. Then (6.13), (6.14), and (6.16) are three linear equations which determine the three coefficients c_1, c_3, and c_5 completely if γ is known. It turns out that with the above assumption γ is the only parameter of our theory which we can tune. Particle-hole symmetry requires that $\rho_0\bar{S}(k)$ is a symmetric function of ν around $\nu=1/2$ where $\rho_0=\nu/2\pi\ell^2$. Equation (6.15) implies that $\gamma=\gamma(\nu)$ must be also symmetric in ν around $\nu=1/2$. Since in our theory we are interested in occupation fractions ν which are not too far away from $\nu=1/2$, we can assume in a lowest order approximation that γ is a constant independent of ν. This assumption implies that the dispersion relation of the mode energies $E(k)$ does not depend on the occupation fraction ν but only on the value of γ. We have varied γ in the interval $0\leq\gamma\leq 3$ and determined the dispersion relation $E(k)$ numerically. We find a magnetoroton minimum at wave numbers $k\approx\ell^{-1}$ that agrees with the results of Ref. 13. For smaller values γ the magnetoroton minimum becomes stronger, while for larger values γ it becomes fainter and disappears for $\gamma\geq 1.5$. We find that for $\gamma=1.0$ the dispersion relation $E(k)$ has the most reasonable form and looks similar like that for $\nu=1/3$ in Ref. 13. Thus, for our purpose $\gamma=1.0$ seems to be the optimal choice. Actually, for the Laughlin ground states with occupation fractions $\nu=1/m$ where $m=3,5,7,\ldots$, the leading-order term (6.15) of the structure factor $\bar{S}(k)$ can be determined exactly,[13,20,21] which implies $\gamma=1/4\nu$. The resulting value of $\gamma=0.75$ for $\nu=1/3$ is very close to our choice.

Now, all we need as input for our theory is complete and we can present our results. In the following calculations we choose the occupation fraction $\nu=1/2$. It turns out that the results are qualitatively similar also for other occupation fractions ν in the interval $0<\nu<1$ not too close to 0 or 1. We choose $\gamma=1.0$, determine c_1, c_3, c_5 via (6.13), (6.14), (6.16), and obtain the structure factor $\bar{S}(k)$ from (6.12). Then we proceed as described above and obtain the bosonic spectral function $B''(\epsilon)$ by (6.1) and (5.23). The result is shown in Fig. 13 as a full line. $B''(\epsilon)$ is the **k** integrated effective spectral function of the collective excitations, which we need as the input for our independent-boson model. As it should be, $B''(\epsilon)$ is antisymmetric in the energy ϵ. One can clearly see that the main spectral weight is located at the energy $0.1e^2/\ell$ (and also at $-0.1e^2/\ell$). In analogy to the sum-rule gap 2Δ (5.17), which can be viewed as the average energy of the spectral weight $\chi''(\epsilon)$ of the pair propagator, we define the average energy of the collective excitations
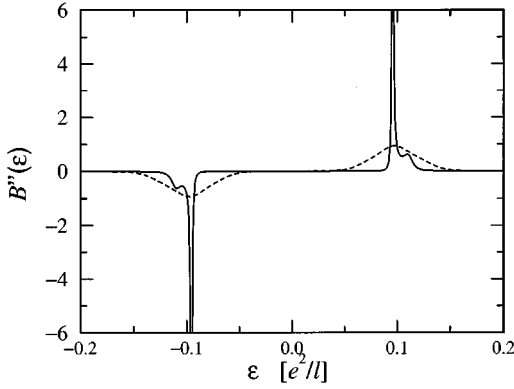
FIG. 13. The spectral function $B''(\epsilon)$ of the **k** integrated collective excitations, defined by (5.23), in single-mode approximation for $\nu = 1/2$ and $T = 0$. The dashed line is the same but with the δ functions in (6.1) replaced by Gaussian peaks of width $\Delta\epsilon = 0.02 e^2/\ell$. The main spectral weight arises from the magnetorotons and is located at the average energy $\bar{E} = 0.099 e^2/\ell$.

$$\bar{E} = \int_0^\infty d\epsilon \; \epsilon B''(\epsilon) \bigg/ \int_0^\infty d\epsilon \; B''(\epsilon) \qquad (6.17)$$

and obtain the value $\bar{E} = 0.099 e^2/\ell$. Since the experiments,[1-3] which we want to explain with our theory, are done at very low temperatures $T \approx 0.01 k_B^{-1} e^2/\ell$ so that $\bar{E}/k_B T \approx 10$, we have performed the calculations of the single-mode approximation at zero temperature. This means in (6.6) we have set $\tanh[(1/2)\beta E(k)] \approx \tanh(5) \approx 1$ in good approximation, so that the spectral weight $a(k)$ of the collective excitations in (6.1) is identified with the structure factor $a(k) = \rho_0 \bar{S}(k)$. It is known that the structure factor $\bar{S}(k)$ of the density projected to the lowest Landau level has its main weight for wave numbers k in the interval $0.5 \ell^{-1} \lesssim k \lesssim 2.5 \ell^{-1}$. On the other hand, the dispersion relation $E(k)$ has a minimum with a positive gap in the same k interval which is called the magnetoroton minimum. Thus we can say that the main contribution of the spectral function $B''(\epsilon)$ comes from the *magnetorotons*.

The single-mode approximation (6.1) is based on the ansatz that the spectrum of the collective excitations with wave number k is a delta function located at the average energy $E(k)$. In reality there are several modes for each k so that the peak of $\chi''_{\rho\rho}(k,\epsilon)$ at $E(k)$ will be smeared out. To take this effect into account to a certain extent, we have replaced the δ functions in (6.1) by Gaussian peaks with a finite width $\Delta\epsilon = 0.02 e^2/\ell$, which is still small compared to the average energy $\bar{E} = 0.099 e^2/\ell$. The resulting spectral function $B''(\epsilon)$ is shown in Fig. 13 as a dashed line. One clearly sees that this spectral function of the **k** integrated collective excitations is much smoother and somewhat more smeared out compared to the full line calculated with δ functions in (6.1), while the average energy $\bar{E}$ is not changed.

We take the spectral function $B''(\epsilon)$ from Fig. 13 and determine $B(\tau)$ via a formula analogous to (2.9). Then we calculate the electronic Green's function $G(\tau - \tau')$ by (5.14) and (4.8) and obtain the electronic spectral function $A(\epsilon)$ by analytic continuation via Padé approximation. The result is shown in Fig. 14, where the full and dashed line correspond to those in Fig. 13 We find what we expect from the experi-
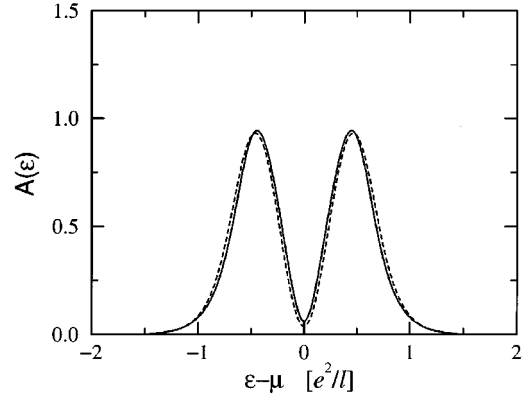

FIG. 14. The electronic spectral function $A(\epsilon)$ for $\nu = 1/2$ and $T = 0.01 k_B^{-1} e^2/\ell$ obtained from (5.14), (4.8), and analytic continuation using $B''(\epsilon)$ of Fig. 13, as input for the collective excitations. The full and dashed line correspond to those in Fig. 13. One clearly sees the double-peak structure with the pseudogap at $\epsilon = \mu$. The symmetry of $A(\epsilon)$ around $\epsilon = \mu$ is a speciality of the occupation fraction $\nu = 1/2$ and reflects particle-hole symmetry.

ments: $A(\epsilon)$ has two peaks separated by a pseudogap at $\epsilon = \mu$ where $\mu = \epsilon_1$ and ϵ_1 is given by (5.12). The left peak with energies $\epsilon < \mu$ represents the hole excitations, and the right peak with energies $\epsilon > \mu$ represents the electron excitations. Here $A(\epsilon)$ is symmetric with respect to $\epsilon = \mu$. This fact is a speciality of the occupation fraction $\nu = 1/2$ and reflects particle-hole symmetry. For other values of ν the spectral function $A(\epsilon)$ is not symmetric. In this case the two peaks have different sizes, but the pseudogap at $\epsilon = \mu$ remains.

From (3.5) or (5.16) we obtain the pair propagator $\chi(\tau - \tau')$ and by analytic continuation the related spectral function $\chi''(\epsilon)$. The result is shown in Fig. 15. Because of (3.6) the spectral function $\chi''(\epsilon)$ is directly related to the current-voltage characteristic $I(V)$ of the tunneling experi-
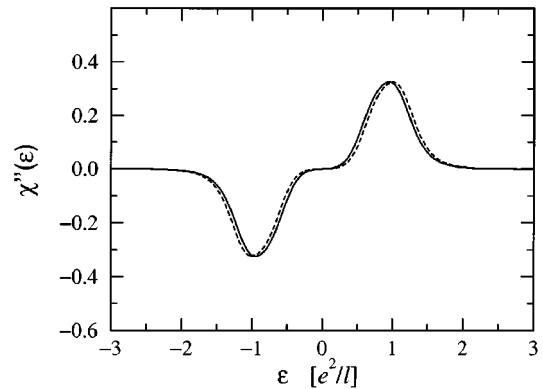

FIG. 15. The spectral function of the pair propagator $\chi''(\epsilon)$ for $\nu = 1/2$ and $T = 0.01 k_B^{-1} e^2/\ell$ obtained from (3.5) or (5.16) and analytic continuation. The full and dashed line correspond to those in Figs. 13 and 14. Equation (3.6) allows us to compare the curve directly with the current-voltage characteristic $I(V)$ by proper rescaling of both axes. Qualitatively our curve agrees quite well with the experimental results in Refs. 1–3. $\chi''(\epsilon)$ is always an antisymmetric function. For positive ϵ we find one broad peak located at the average energy $2\Delta \approx 1.0 e^2/\ell$ and a tunneling pseudogap at small energies (voltages).

ment by rescaling the two axes. Thus, we can easily compare our curve in Fig. 15 with the experimental results[1–3] by changing the variables and hence the scale on the two axes. Qualitatively we find very good agreement with the experiments. Our curve has nearly the same shape as the experimental curve. For $\chi''(\epsilon)$ [and hence for $I(V)$] we find one broad peak at a certain energy (voltage) and a tunneling pseudogap at small energies (voltages) as it is in the experiments. The scale of the horizontal axis in Fig. 15 is determined by the sum-rule gap 2Δ as energy scale, which according to (5.17) can be interpreted as average energy calculated with $\chi''(\epsilon)$ as weight function,

$$2\Delta = \int_0^\infty d\epsilon \, \epsilon \chi''(\epsilon) \Big/ \int_0^\infty d\epsilon \, \chi''(\epsilon). \qquad (6.18)$$

In the single-mode approximation 2Δ is most easily evaluated by (5.18) using (6.9), which yields

$$2\Delta = \int \frac{d^2k}{(2\pi)^2} \frac{2a(k)}{E(k)} [V(k)]^2 e^{-k^2\ell^2/2}. \qquad (6.19)$$

From this formula we obtain the values $2\Delta = 0.96e^2/\ell$ and $1.01e^2/\ell$ for the full and dashed line, respectively, and for $\nu = 1/2$, which can be clearly identified as the average peak position of $\chi''(\epsilon)$ in Fig. 15. In a recent paper[9] the sum-rule gap 2Δ has been related exactly to the ground-state energy. Using an interpolation formula for the ground-state energy the value $2\Delta_{\text{exact}} \approx 0.6e^2/\ell$ has been found for $\nu = 1/2$, which is very accurate and can be viewed as nearly exact. The experimental result[1,3] $2\Delta_{\text{exp}} \approx 0.5e^2/\ell$ is even somewhat smaller. Thus it turns out that our sum-rule gap is by a factor of 1.6 or 1.9 too large compared to the exact or measured value, respectively. However, since our theory contains a lot of approximations which imply that the originally microscopic theory is drastically reduced to an independent-boson model, we cannot expect that our theory yields a quantitatively correct value for the sum-rule gap 2Δ. On the other hand, our value for 2Δ has the right order of magnitude, so that the disagreement is not so bad.

In our theory the effect of the collective excitations (magnetorotons) on the electronic Green's function (5.14) is included in the function $\Delta\Phi(\tau)$ in the exponent. We have calculated this function numerically by (4.8) and find that $\Delta\Phi(\tau)$ is negative in the open interval $0 < \tau < \hbar\beta$ and zero at its boundaries $\tau = 0$ and $\tau = \hbar\beta$. For very low temperatures $T \ll k_B^{-1}\bar{E}$ the interval $0 < \tau < \hbar\beta = \hbar/k_BT$ becomes very large, and it turns out that $\Delta\Phi(\tau)$ is mainly constant in the inner part of the interval. We approximately find the value

$$\Delta\Phi(\tau) \approx -\Delta/\bar{E} \quad \text{for} \quad \hbar/\bar{E} \lesssim \tau \lesssim \hbar\beta - \hbar/\bar{E}. \qquad (6.20)$$

[This value is obtained if we approximate the bosonic spectral function $B''(\epsilon)$ by two delta peaks located at energies $+\bar{E}$ and $-\bar{E}$. For $T \to 0$ the exact value is the spectral moment $-\int_0^\infty d\epsilon B''(\epsilon)/\epsilon^2$.] This fact implies that $G(\tau)$ in (5.14) is nearly a free fermion Green's function in the inner part of the τ interval, but scaled with the exponential factor $e^{-\Delta/\bar{E}}$. By analytic continuation we find the implication on the electronic spectral function, which is

$$A(\epsilon) = e^{-\Delta/\bar{E}}\delta(\epsilon - \epsilon_1) + \text{regular terms} \qquad (6.21)$$

in the zero-temperature limit where $\mu = \epsilon_1$ and ϵ_1 is given by (5.12). While we identify the regular terms with the two broad peaks in Fig. 14, the delta function causes a sharp peak at $\epsilon = \mu$. However, this sharp peak is strongly suppressed by the exponential factor $e^{-\Delta/\bar{E}}$. We believe that the δ peak in (6.21) is an artifact of the independent-boson model, which should not be present in an exact theory. At least for the fractional-quantum-Hall-effect fractions $\nu = p/q$ there is no δ peak because $A(\epsilon)$ has a real gap. (For other occupation fractions ν this is not proven so that in general we cannot exclude the existence of a small δ peak.) Thus for the validity of our theory the weight factor $e^{-\Delta/\bar{E}}$ of the δ peak must be negligibly small. This means that the ratio $\Delta/\bar{E}$, the quotient of the average energy Δ of the single-particle excitations ($=$ half of the sum-rule gap) and the average energy of the collective excitations (magnetorotons) should be large. From our values of 2Δ and $\bar{E}$ we obtain the ratio $\Delta/\bar{E} = 5.0$ for $\nu = 1/2$, which implies a sufficiently small weight factor $e^{-\Delta/\bar{E}} \approx 0.007$ of the δ peak. Indeed, we have found out from our numerical calculations that the ratio $\Delta/\bar{E}$ should be about 5 or larger to observe the double-peak structure with a pseudogap in the electronic spectral function.

Inserting (6.20) into (5.16) we find that in the inner part of the τ interval $\chi(\tau)$ is the free pair propagator scaled by the exponential factor $e^{-2\Delta/\bar{E}}$. By analytic continuation we obtain the implication on the spectral function $\chi''(\epsilon)$, which is

$$\chi''(\epsilon) = \nu(1-\nu)e^{-2\Delta/\bar{E}}\epsilon\delta(\epsilon) + \text{regular terms.} \qquad (6.22)$$

Actually, in this function the singular term vanishes because the extra factor ϵ implies $\epsilon\delta(\epsilon) = 0$. On the other hand, the weight factor $e^{-2\Delta/\bar{E}}$ is the square of the weight factor of the delta function in $A(\epsilon)$ and hence much smaller. Thus, a singular behavior at $\epsilon = 0$ in $\chi''(\epsilon)$ and hence at $V = 0$ in the current-voltage characteristic $I(V)$, which could arise as an artifact of the independent-boson model, does not appear. In Fig. 15 one clearly sees that $\chi''(\epsilon)$ is smooth at $\epsilon = 0$.

In our theory, which is an independent-boson model combined with the single-mode approximation for the magnetorotons, we have one parameter that we can tune: the coefficient γ of the leading term of the structure factor $\bar{S}(k)$ in (6.15). Our optimal choice is $\gamma = 1.0$ (used for the curves in Figs. 13–15). We have performed our calculations also for other values of γ. If γ is decreased, then $\bar{E}$ becomes somewhat larger and Δ somewhat smaller. The ratio $\Delta/\bar{E}$ decreases, and the peak of the current-voltage characteristic $I(V)$ or of $\chi''(\epsilon)$ becomes somewhat broader while the tunneling pseudogap at small V or ϵ becomes smaller. For smaller γ we soon get troubles with the δ peak in $A(\epsilon)$ because the exponential factor $e^{-\Delta/\bar{E}}$ is not small enough. On the other hand, if γ is increased, then $\bar{E}$ becomes somewhat smaller and Δ larger. The ratio $\Delta/\bar{E}$ increases and can be made easily as large as 100 if we choose $\gamma = 4.5$. The peak of $I(V)$ or $\chi''(\epsilon)$ becomes sharper while the tunneling pseudogap becomes somewhat larger. In the ultimate limit

$\Delta/\bar{E}\rightarrow\infty$ where $\bar{E}\rightarrow0$ and Δ is kept fixed, the peaks of $I(V)$, $\chi''(\epsilon)$, and $A(\epsilon)$ become δ functions for $T=0$. This limiting case has been considered at the end of Sec. V. The related spectral function $A(\epsilon)$ is given by (5.22) in the limit $\delta\rightarrow0$ for $T=0$. Comparing $\chi''(\epsilon)$ with the experimental curve of $I(V)$ we find by considering the shape of the curves and especially the ratio of the peak width to the tunneling pseudogap, that $\Delta/\bar{E}\approx5$ and hence $\gamma\approx1.0$ are the optimal values.

Surprisingly the differences between the dashed line and the full line of $A(\epsilon)$ and $\chi''(\epsilon)$ in Figs. 14 and 15, respectively, are very small, while in Fig. 13 the differences for the spectrum of the collective excitations $B''(\epsilon)$ are quite large. We remember that the dashed line in Fig. 13 has been calculated by smearing out the δ functions in the single-mode approximation (6.1) by Gaussian peaks of width $\Delta\epsilon=0.02e^2/\ell$. While the average energy $\bar{E}=0.099e^2/\ell$ of the collective excitations remains fixed, smearing out the spectrum $B''(\epsilon)$ causes a slight enhancement of the sum-rule gap 2Δ from $0.96e^2/\ell$ (full line) to $1.01e^2/\ell$ (dashed line), which means that the peaks of $A(\epsilon)$ and $\chi''(\epsilon)$ are shifted a little bit to higher energies. This effect, however, is very small. Thus we arrive at the conclusion that the precise shape of the spectrum of the collective excitations (magnetorotons) $B''(\epsilon)$ has nearly no influence on the shape of the curves of $A(\epsilon)$, $\chi''(\epsilon)$, and $I(V)$. The qualitative form of the current-voltage characteristic $I(V)$ is mainly determined by the parameters 2Δ, $\bar{E}$, and the temperature T.

In our calculations the parameters have the values $T=0.01k_B^{-1}e^2/\ell$, $\bar{E}\approx0.1e^2/\ell$, and $2\Delta\approx1.0e^2/\ell$, which means that we have the inequality $k_BT\ll\bar{E}\ll2\Delta$ where each inequality sign means a factor of about 10. We have also changed the temperature. Once the temperature is $T=0.1k_B^{-1}\bar{E}$ or below, the pseudogaps of $A(\epsilon)$ and $\chi''(\epsilon)$ are visible, and the curves nearly do not change any more if the temperature is lowered more or if it is even $T=0$. Hence the curves in Figs. 14 and 15, which are calculated for $T=0.01k_B^{-1}e^2/\ell$, represent nearly zero-temperature results. If the temperature comes close to $T\approx k_B^{-1}\bar{E}$ or higher, the pseudogaps of $A(\epsilon)$ and $\chi''(\epsilon)$ vanish. Eventually, $A(\epsilon)$ becomes a single broad peak if $T\gg k_B^{-1}\bar{E}$.

The results shown in Figs. 14 and 15 are obtained for the occupation fraction $\nu=1/2$. We have performed the calculations also for other values of ν. The most drastic changes are observed in $A(\epsilon)$. While the double-peak structure and the pseudogap at $\epsilon=\mu$ remains, the sizes of the two peaks change and $A(\epsilon)$ is no more symmetric around $\epsilon=\mu$. On the other hand, the changes of $\chi''(\epsilon)$ and hence of the current-voltage characteristic $I(V)$ are small, if ν does not come too close to 0 or 1. This observation agrees with the experimental finding,[1-3] that the influence of the occupation fraction ν on $I(V)$ is small. Especially, nothing unusual is seen at the rational fractions $\nu=p/q$ of the fractional quantum Hall effect. For $\nu=1/3$ we have performed the calculations using the results of the single-mode approximation for $\bar{S}(k)$ and $E(k)$ of Ref. 13 (the coefficients c_m of Table I therein). The resulting $\chi''(\epsilon)$ is very similar to the curve in Fig. 15, while we find $2\Delta=0.97e^2/\ell$, $\bar{E}=0.091e^2/\ell$, and $\Delta/\bar{E}=5.3$,

which are values similar to those given above. This fact tells us that our interpolation of the structure factor $\bar{S}(k)$ seems to be good.

We have performed the numerical calculations to obtain the curves in Figs. 14 and 15 by using the Matsubara formalism and analytic continuation to real frequencies. It is well known that sometimes the analytic continuation is problematic and does not yield the correct results for the spectral functions. Thus we have performed the numerical calculations also with the Keldysh formalism, which deals directly with spectral functions and avoids the analytic continuation. We have found nearly the same results for $A(\epsilon)$ and $\chi''(\epsilon)$, so we can be sure that our curves in Figs. 14 and 15 are quite accurate.

VII. CONCLUSIONS

We have investigated the two-dimensional strongly correlated electron system in the fractional quantum Hall regime on a microscopic level using many-particle quantum-field theory. Due to the degeneracy of the lowest Landau level, standard perturbation theory fails at low temperatures. The perturbation series can be improved by resummation of self-energy subdiagrams, which yields the self-consistent quantum-field theory. While this self-consistent theory works successfully for superconductivity,[17] it fails for the fractional quantum Hall system too, because all Feynman diagrams have the same order.

To solve the problem, we have proposed a resummation procedure for the electron Green's function, which, after a certain approximation, ends up exactly in the solution of an independent-boson model. To do this we separate a bosonic part with zero wave vector from the interaction, which can be treated exactly, and obtain a transformation formula for the electron Green's function that represents a resummation of Feynman diagrams and goes beyond perturbation theory. The separated bosonic interaction part plays the role of the "independent bosons" and is identified with the collective excitations. Since our method yields no resummation for the density-density correlation function, we cannot calculate this correlation function by field-theoretic means. A more sophisticated theory for the collective excitations, which is called the single-mode approximation, has been developed by Girvin, MacDonald, and Platzman.[13] Using this method we determine the **k** integrated spectrum of the collective excitations, which we need as an input for the independent-boson model. It turns out that the main spectral weight comes from the magnetorotons.

Thus, our theory is a combination of an independent-boson model with the single-mode approximation. We calculate the electronic Green's function and obtain from this the electronic spectral function $A(\epsilon)$. The result is a spectral function with a double-peak structure with a pseudogap at $\epsilon=\mu$ (see Fig. 14). By a convolution (1.1) of the spectral function $A(\epsilon)=A_+(\epsilon)+A_-(\epsilon)$ the current-voltage characteristic $I(V)$ for the tunneling between two fractional quantum Hall layers is obtained that is directly related to the spectral function of the pair propagator $\chi''(\epsilon)$ by (3.6). Our result for $I(V)$ (see Fig. 15) shows a strong suppression (tunneling pseudogap) for small voltages at low temperatures and agrees qualitatively quite well with the experiments.[1-3]

The voltage scale is ruled by the sum-rule gap[9] 2Δ. Our value is by a factor 1.6 or 1.9 too large compared to the exact and experimental value. Since our theory contains many approximations, this disagreement is not so bad. It turns out that the shape of the curves of $\chi''(\epsilon)$ and $I(V)$ is mainly determined by the ratio between the characteristic energy of the single-particle excitations Δ and the average energy $\bar{E}$ of the collective excitations (magnetorotons), while the precise shape of the collective-excitation spectrum has nearly no influence. We obtain the value $\Delta/\bar{E} \approx 5$, which is also required by the independent-boson model to produce a curve that qualitatively agrees with the measured $I(V)$.

Our theory explains the observations of the two-layer tunneling experiments as an effect of the electronic correlations in a *single layer*, while the interlayer interactions are neglected. It supports the qualitative picture for the origin of the pseudogap described already in Ref. 1, that a tunneled electron and the created hole must emit collective excitations to relax and build up the correlations with the surroundings.

Furthermore, our theory supports the approach of Johansson and Kinaret[5] on a microscopic level. These authors have constructed an independent-boson model directly by considering the tunneling process of one electron and modeling the surroundings by *magnetophonons* as the collective excitations in a Wigner crystal. The main progress of our method is that we derive the independent-boson model from the microscopic theory by a certain approximation, while the collective excitations are the *magnetorotons* of a liquid state in the fractional quantum Hall regime.

*On leave from Sektion Physik der Ludwig-Maximilians-Universität München, Theresienstrasse 37, D-80333 München, Germany.

[1] J. P. Eisenstein, L. N. Pfeiffer, and K. W. West, Phys. Rev. Lett. **69**, 3804 (1992); Surf. Sci. **305**, 393 (1994).

[2] J. P. Eisenstein, L. N. Pfeiffer, and K. W. West, Phys. Rev. Lett. **74**, 1419 (1995).

[3] K. M. Brown, N. Turner, J. T. Nicholls, E. H. Linfield, M. Pepper, D. A. Ritchie, and G. A. C. Jones, Phys. Rev. B **50**, 15 465 (1994); N. Turner, J. T. Nicholls, K. M. Brown, E. H. Linfield, M. Pepper, D. A. Ritchie, and G. A. C. Jones (unpublished).

[4] R. C. Ashoori, J. A. Lebens, N. P. Bigelow, and R. H. Silsbee, Phys. Rev. Lett. **64**, 681 (1990); Phys. Rev. B **48**, 4616 (1993).

[5] P. Johansson and J. M. Kinaret, Phys. Rev. Lett. **71**, 1435 (1993); Phys. Rev. B **50**, 4671 (1994).

[6] See G. D. Mahan, *Many-Particle Physics* (Plenum, New York, 1981), Chap. 4.

[7] A. L. Efros and F. G. Pikus, Phys. Rev. B **48**, 14 694 (1993).

[8] Y. Hatsugai, P.-A. Bares, and X. G. Wen, Phys. Rev. Lett. **71**, 424 (1993); S. He, P. M. Platzman, and B. I. Halperin, *ibid.* **71**, 777 (1993).

[9] R. Haussmann, H. Mori, and A. H. MacDonald, Phys. Rev. Lett. (to be published).

[10] I. L. Aleiner, H. U. Baranger, and L. I. Glazman, Phys. Rev. Lett. **74**, 3435 (1995).

[11] A. A. Abrikosov, L. P. Gorkov, and I. E. Dzyaloshinskii, *Methods of Quantum-Field Theory in Statistical Physics* (Dover, New York, 1963).

[12] A. L. Fetter and J. D. Walecka, *Quantum Theory of Many-Particle Systems* (McGraw Hill, New York 1971).

[13] S. M. Girvin, A. H. MacDonald, and P. M. Platzman, Phys. Rev. Lett. **54**, 581 (1985); Phys. Rev. B **33**, 2481 (1986).

[14] L. Zheng and A. H. MacDonald, Surf. Sci. **305**, 101 (1994).

[15] T. Matsubara, Prog. Theor. Phys. **14**, 351 (1955).

[16] J. M. Luttinger and J. C. Ward, Phys. Rev. **118**, 1417 (1960).

[17] R. Haussmann, Z. Phys. B **91**, 291 (1993); Phys. Rev. B **49**, 12 975 (1994).

[18] L. V. Keldysh, Zh. Éksp. Teor. Fiz. **47**, 1515 (1964) [Sov. Phys. JETP **20**, 1018 (1965)].

[19] J. Rammer and H. Smith, Rev. Mod. Phys. **58**, 323 (1986).

[20] J. M. Caillol, D. Levesque, J. J. Weis, and J. P. Hansen, J. Stat. Phys. **28**, 325 (1982).

[21] R. B. Laughlin, in *Proceedings of the Seventeenth International Conference on Low-Temperature Physics*, edited by U. Eckern, A. Schmid, W. Weber, and H. Wühl (North Holland, Amsterdam, 1984).